Applied Geochemistry 169 (2024) 106015

Contents lists available at ScienceDirect

Applied Geochemistry

journal homepage: www.elsevier.com/locate/apgeochem

Degradation of the polyacrylonitrile-based UP2W material under cementitious conditions

A. Tasi [a,**,1], P. Szabo [a], X. Gaona [a,*], M. Bouby [a], T. Sittel [a], D. Schild [a], A.C. Maier [b], S. Hedström [b], M. Altmaier [a], H. Geckeis [a]

[a] Karlsruhe Institute of Technology, Institute for Nuclear Waste Disposal, P.O. Box 3640, 76021, Karlsruhe, Germany
[b] Svensk Kärnbränslehantering AB, Evenemangsgatan 13, Box 3091, 169 03, Solna, Sweden

ARTICLE INFO

Editorial handling by Dr Erich Wieland

Keywords:
Polyacrylonitrile
UP2W
Alkaline degradation
Cement
Degradation products
Radioactive waste

ABSTRACT

UP2W is a polyacrylonitrile-based filter aid material used in nuclear power plants, which is disposed in repositories for low and intermediate level radioactive waste. The degradation of UP2W was investigated in a series of batch experiments in the presence and absence of portlandite, Fe(0) and NaOH, which simulate the hyperalkaline, reducing conditions expected in repositories with cementitious engineered barriers. Degradation experiments were performed under Ar atmosphere at $T = 22$ or 80 (± 2) °C. Aliquots of the supernatant solutions and retrieved solid phases were systematically characterized for *ca.* 5 years using a multi-method approach.

The evolution of dissolved organic carbon shows a strong contrast between NaOH- and $Ca(OH)_2$-buffered systems. In the absence of Ca, an early, sharp increase in the dissolved organic carbon is observed, and its magnitude correlates with the initial NaOH concentration.

In $Ca(OH)_2$-buffered systems, dissolved organic carbon remained very low (<10 ppm) up to 600 days, but steadily increased afterwards reaching ~ 50 ppm at $t \approx 1800$ days. Size-exclusion/liquid chromatography coupled with organic carbon, ultra-violet and organic nitrogen detection (LC-OCD-UVD-OND) confirmed the presence of significantly smaller fragments in solution compared to NaOH-systems, which however were found to increase with time.

Overall observations underline that hydrolysis of the nitrile functional groups, chain scission of the polymer backbone and cross-linking of polymer fragments in the degradation leachates play a key role in the progress of the degradation reaction. Chain scission is hindered in the presence of Ca, possibly due to the complexation of Ca with amide and carboxylate intermediates and the consequent decrease in electron density on the β-carbon atoms. This study improves the mechanistic understanding and quantitative description of UP2W degradation in cementitious environments relevant for L/ILW disposal.

1. Introduction

The accurate prediction of radionuclide transport in the context of nuclear waste disposal strongly relies on aqueous chemical parameters. The solubility and sorption properties of radionuclides correlate with their aqueous speciation, which can be importantly affected by the presence of inorganic and organic complexing ligands.

Organic materials are disposed in large quantities alongside low- and intermediate-level radioactive waste (L/ILW) in underground disposal facilities such as SFR, the final repository for short-lived L/ILW in Sweden (Keith-Roach et al., 2021). Cementitious materials are extensively used in repositories for L/ILW for the stabilization of the waste and for construction purposes, acting as barrier against groundwater flow and radionuclide transport (Ochs et al., 2016; Wieland, 2014). Upon contact with groundwater, cementitious materials will buffer the pore water composition to highly alkaline pH and moderate Ca concentrations. Three main stages are usually considered to describe the evolution of cement degradation: (i) stage I involves the leaching of the highly soluble Na_2O/K_2O, and is characterized by high pH and concentration of alkalis (pH > 13; [Na + K] ≈ 0.3–0.5 M), (ii) stage II is

* Corresponding author.
** Corresponding author.
E-mail addresses: agost.tasi@framatome.com (A. Tasi), xavier.gaona@kit.edu (X. Gaona).
[1] Current address: Framatome GmbH, Erlangen, Germany.

https://doi.org/10.1016/j.apgeochem.2024.106015
Received 26 January 2024; Received in revised form 8 April 2024; Accepted 25 April 2024
Available online 3 May 2024

governed by portlandite ($Ca(OH)_2$) dissolution, which buffers the pore water composition at pH ≈ 12.5 and [Ca] ≈ 20 mM, (iii) stage III entails the incongruent dissolution of C–S–H with decreasing Ca:Si ratio and pH (~12.5 → ~ 10). Moreover, the anoxic corrosion of Fe present in the repository as waste and construction materials, will result in the generation of hydrogen, thus defining strongly reducing conditions. Under these conditions, organic materials may undergo degradation, particularly involving hydrolysis triggered by the dominating hyperalkaline conditions. Cellulose, for instance, is known to decompose through hydrolytic reactions to (mainly, but not exclusively) isosaccharinic acids, which are capable of forming relatively stable complexes with actinides, lanthanides and transition metals under alkaline, reducing conditions potentially affecting their solubility and sorption properties (González-Siso et al., 2018; Hummel et al., 2005; Rai and Kitamura, 2017; Tasi et al., 2018a, 2018b; Tits and Wieland, 2018; Tits et al., 2005; Vercammen et al., 2001).

UP2W is a filter aid support material used for ion-exchange resins in various operations in nuclear power plants (Abdel Rahman et al., 2018; Brost, 1974; Sebesta et al., 1996), and it is accordingly disposed in specific waste streams in L/ILW (Duro et al., 2012; Keith-Roach et al., 2021). UP2W is a commercial polymeric compound consisting of 20–40 w% of polyacrylonitrile (PAN), 60–80 w% of water and <0.5 w% of N, N-dimethylacetamide (UP2W, 2017).

The thermal decomposition of PAN has been previously studied due to its applications in carbon fiber production (Föchler et al., 1985; Martin et al., 2001; Mathur et al., 1992; Surianarayanan et al., 1998). A large number of publications also deal with the alkaline modification of the fiber mass to produce superadsorbents for scavenging hazardous ions from drinking water (Chaudhary and Farrell, 2014; Deng et al., 2003), accordingly providing an extensive basis to understand the degradation mechanism of PAN under various alkaline conditions (Bajaj et al., 1985; Bashir et al., 1991; Batty and Guthrie, 1981; Ermakov et al., 2000; Glazkovskii and Mikhailov, 1966; Kudryavtsev et al., 2000; Litmanovich and Platé, 2000). However, the available literature on the evolution of its dissolution process under alkaline conditions, *i.e.* the hydrolytic depolymerization and fragmentation of the material, is scarce (Dario et al., 2004; Duro et al., 2012; Holgersson et al., 2011; Tasdigh, 2015).

According to the most comprehensive summary on the hydrolytic degradation mechanism of PAN published by (Litmanovich and Platé, 2000), the process is initiated by the nucleophilic attack of OH^- ions on the nitrile carbon atoms. This step promotes the formation of conjugated structures, cyclic amidines, to a certain extent. These poly-conjugates are prone to further hydrolyze through nucleophilic attack on their amidine carbon atoms by hydroxide ions, leading to the generation of carboxylates, amidines and NH_3. The length of these conjugated structures is strongly affected by temperature and the presence of impurities, as their formation can be viewed as the competition between two processes. Potentially, intermediates can undergo tautomerization reactions to form an amide and a lower poly-conjugate amidine structure. Finally,

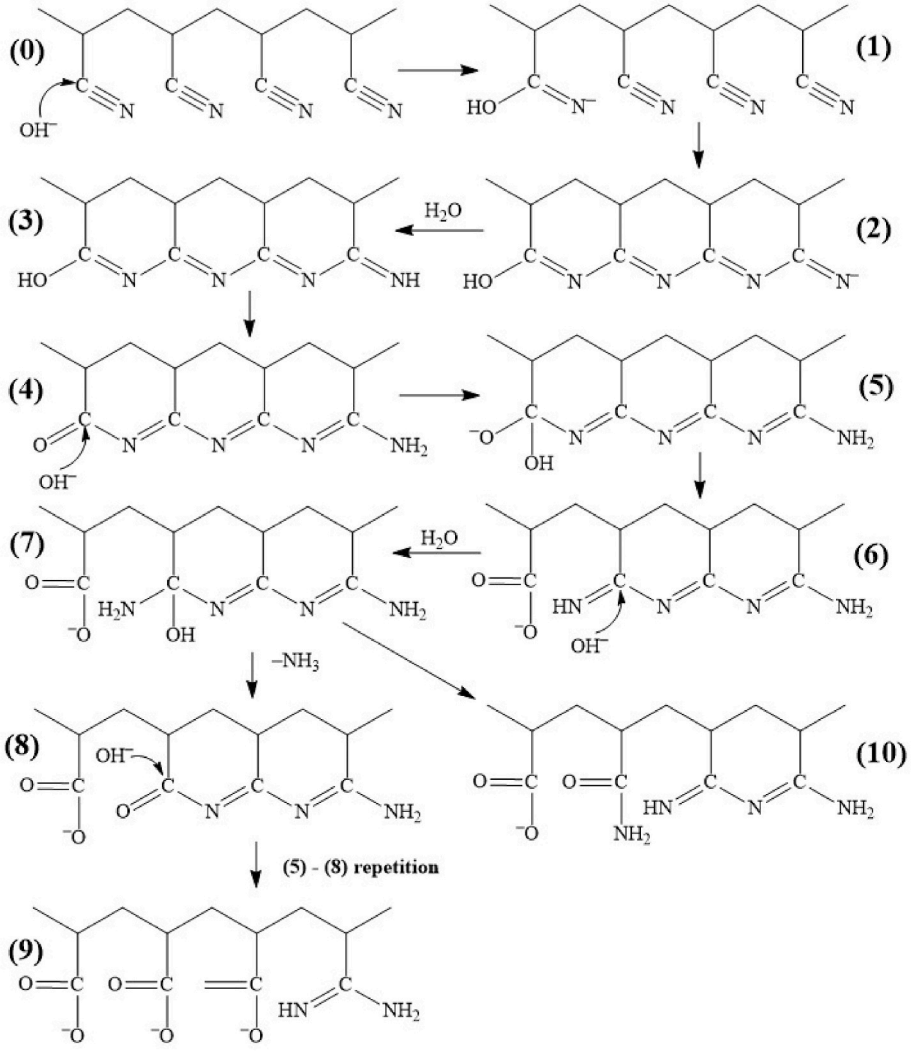

Fig. 1. Scheme described by Litmanovich and Platé for the hydrolysis of PAN (Litmanovich and Platé, 2000).

amides and amidines eventually experience further hydrolysis through nucleophilic attack on their carbon atoms by OH^- ions to form carboxylates as the final functional groups, again involving the release of NH_3. A scheme of the mechanism proposed by (Litmanovich and Platé, 2000) is shown in Fig. 1. (Bashir et al., 1991) observed a gelation process with time under alkaline conditions, confirmed by the increase in viscosity measured on dilute solutions of the polymer. They proposed that an azomethine cross-linking took place, where the resonance-stabilized carbanion generated by the abstraction of the methine proton attacked the nitrile carbon on another polymer chain to form a primary imine with a linked structure across the two carbon chains. The methine proton abstraction and the existence of the given carbanion was also underlined by the authors through investigating the effect of deuterization on ^{13}C NMR spectra. It was identified as the main intermediate responsible for changing the tacticity of the polymeric chain through inversion and also for the scission of the carbon chain.

Note that the chain scission, *i.e.* depolymerization, is the key process leading to the potential formation of smaller (soluble) polymeric fragments, which may affect the retention of radionuclides in the context of a repository for L/ILW. Experimental studies focusing on the hydrolytic fragmentation of UP2W under alkaline conditions are limited and to a significant degree not consistent with each other in terms of dissolution rate, effect of Ca ions and temperature, or the type of low molecular weight ligands generated through the degradation process (Dario et al., 2004; Duro et al., 2012; Holgersson et al., 2011; Tasdigh, 2015). This raises relevant uncertainties on the long-term prediction of the degradation products forming and their possible impact on the retention of radionuclides.

(Dario et al., 2004) investigated the degradation of UP2W under alkaline conditions by monitoring the dissolved organic content, and studied the effect of the generated leachates on the uptake of Eu(III) by cement and TiO_2. Based on this work, (Duro et al., 2012) continued the investigation with more emphasis on the identification of the UP2W degradation products. These authors studied the degradation of UP2W using 4 different batch samples. At room temperature, two samples were continuously stirred under different conditions: (1) buffered by Ca$(OH)_2$ at pH = 12.5, and (2) buffered by $Ca(OH)_2$ at pH = 13.4. Two additional experiments were equilibrated at $T = 60$ °C, with pH adjusted to 12.5 with NaOH, (3) in the absence of Ca, and (4) at $[Ca]_{tot} = 0.01$ M UP2W was present in all samples at S:L = 50 g dm^{-3}. The authors observed a slow dissolution process in the room temperature samples with TOC values at $t = 693$ days reaching the level of ~6 and 30 ppm in the pH = 12.5 and 13.4 samples, respectively. For the systems equilibrated at $T = 60$ °C the authors reported significantly higher TOC values (900 and 1400 ppm respectively for samples in the absence and presence of Ca), thus concluding that both elevated temperature and the presence of Ca enhance the rate of UP2W dissolution. The authors identified several short and long carbon-chained mono- and dicarboxylic acids (*e.g.*, 3-hydroxybutanoic acid (MW = 104.10 g), adipic acid (MW = 146.14 g), malonic acid (MW = 104.06 g), decanoic acid (MW = 172.26 g), dodecanoic acid (MW = 200.32 g)) as well as phenyl-derivates and ketones (*e.g.*, 4-phenyl-3-buten-2-one (MW = 146.19 g), 1,5-diphenyl-1, 4-pentadien-3-one (MW = 234.30 g), 1,5-diphenyl-1-penten-3-one (MW = 236.31 g), 2-octanone (MW = 128.22 g)), but concluded that none of the compounds identified had any direct structural relationship to the original PAN material and thus that the source of these compounds could be related with the unknown additives present in UP2W.

(Holgersson et al., 2011) investigated the dissolution of UP2W at room temperature in fresh cement pore water (FCPW) and leached cement pore water (LCPW). UP2W was introduced at S:L = 24 g dm^{-3} in both systems. Dissolved organic content from UP2W in LCPW reached ~28 ppm and ~40–45 ppm after 319 and 1195 days of contact time, respectively. As for the FCPW system, NPOC levels were around 30 ppm and ~145–166 ppm after 300 and 1195 days of contact time, respectively. These NPOC values are significantly higher than those reported by (Duro et al., 2012) under similar experimental conditions.

In a more recent study, (Tasdigh, 2015) investigated the degradation and dissolution of UP2W under cementitious conditions and the impact of the resulting leachates on the sorption behavior of Ni(II) and Eu(III). Similarly to (Duro et al., 2012), the author conducted two degradation experiments with UP2W at S:L = 25 g dm^{-3}, at room temperature under N_2 atmosphere: (1) buffered by $Ca(OH)_2$ with S:L = 10 g dm^{-3} to pH = 12.5, with the addition of 14 mM of NaOH and 180 mM of KOH, and (2) at pH = 13.4, also containing $Ca(OH)_2$ with S:L = 10 g dm^{-3}, 114 mM NaOH and 180 mM KOH. One additional batch experiment was conducted at $T = 60$ °C with analogous conditions as sample (1) but with UP2W present at S:L = 50 g dm^{-3}. After 6 months of equilibration time, the authors reported TOC values of 1000 and 5000 ppm for the degradation experiments at room temperature with pH = 12.5 and 13.4, respectively. These values are approximately 200 times higher than those reported by Duro et al. under comparable conditions. The TOC content in the degradation experiment at $T = 60$ °C was ~1000 ppm, although the authors reported a significant drop in pH (from 12.5 to 9.3), which was attributed to the complete dissolution of the $Ca(OH)_2$ added at S:L = 10 g dm^{-3}. Note that the high TOC values reported by Tasdigh may be caused by the leaching of organic compounds from the cellulose-acetate filters, but this possible contribution was not discussed by the author.

An accurate quantitative description of the UP2W degradation kinetics is so far missing under the boundary conditions expected in repositories for L/ILW. This hinders long-term predictions on the impact of this organic material in the retention properties of radionuclides. Moreover, in spite of the extensive literature dedicated to the characterization of degraded PAN, only a limited number of studies have inconclusively tackled the characterization of the soluble species generated in this process. In this context, the present work aims at a long-term characterization of the UP2W degradation under conditions relevant for cementitious systems, with focus on the quantification of the dissolved organic content (in terms of NPOC values) as well as the thorough characterization of the soluble leachates and degraded UP2W solid material. This study was performed within the Work Package 3 CORI (Cement-Organic-Radionuclide-Interaction) of the EURAD EU project, in the context of an on-going collaboration between Karlsruhe Institute for Technology—Institute for Nuclear Waste Disposal (KIT-INE) and the Swedish Nuclear Fuel and Waste Management Co. (SKB). The work presented here was developed within Task 2 of CORI, dedicated to the degradation of organic materials expected in repositories for L/ILW.

2. Experimental

All experiments were prepared, stored and conducted at $T = (22 \pm 2)$ °C in gloveboxes under Ar-atmosphere with O_2 concentration below 2 ppm, except where otherwise indicated.

2.1. Chemicals

All solutions were prepared with ultra-pure water purified with a Milli–Q apparatus (Millipore, 18.2 MΩ, 22 ± 2 °C) and purged for several hours at $T = 80$ °C with Ar before use. $Ca(OH)_2$ (EMSURE®, p.A.), Fe (0) (≥99.5 %, powder, $d_p = 10$ μm), $NaHCO_3$ (EMSURE®, p.A.), $Na_2HPO_4 \bullet H_2O$ (Supelco™, LiChropur®), NaOH (Tritrisol®), HCl (Tritrisol® and 30%, Supelco™, Ultrapur) and KH_2PO_4 (Millipore) were obtained from Merck. The UP2W material was provided as fine powder by SKB, originally purchased from Aqua Chem srl (UP2W, 2017). The UP2W formulation consists of 20–40 w% of polyacrylonitrile (PAN), 60–80 w% of water and <0.5 w% of N,N-dimethylacetamide. We note that the formulation of the UP2W material until 2010 included as well 3.5% of additives (anticaking). KH-Phtalate ($C_6H_5C_2O_2O_2K$, BioXtra, ≥99.95 %) was purchased from Sigma-Aldrich. Polystyrene sulfonate (PSS) and poly (acrylic acid) sodium salts (PAA) of different sizes used for the calibration in the size exclusion/liquid chromatography were obtained from Polymer Standards Service and Fluka Chemie GmbH, respectively.

In order to remove carbonate impurities, commercial $Ca(OH)_2$ was heated up to 900 °C in an oven over night and stored in an Ar-glovebox after cooling down to room temperature. Before use, Fe(0) powder was soaked in 0.1 M HCl for 30 min to remove potential outer oxide layer and other impurities (Bruno et al., 2018; Yalcintas et al., 2015), and thus gain more stable readings in the course of the E_h measurements.

2.2. Measurement of pH and E_h

The total concentration of free protons in solution were measured with combination pH electrodes (type Orion Ross, Thermo Scientific), freshly calibrated against standard pH buffers (pH = 3–13, Merck).

The redox potential was determined with a Pt electrode combined with Ag/AgCl reference electrode (Metrohm). Measured potentials were converted to E_h (*versus* standard hydrogen electrode: SHE) by correcting for the potential of the Ag/AgCl inner-reference electrode with 3 M ($mol{\cdot}dm^{-3}$) KCl and T = 22 °C (+207 mV). E_h values were finally converted to the negative logarithm of electron activity (pe = –log a_e–) as $E_h = -RT \ln(10) F^{-1} \log a_{e-}$, where R is the ideal gas constant (8.3145 J $mol^{-1} K^{-1}$) and F is the Faraday constant (96,485.3 C mol^{-1}). E_h values of the solutions were collected following the protocol described by (Altmaier et al., 2010), involving approximately 15 min of measuring time. E_h values of the sample containing Fe(0) were collected under rigorous stirring to promote the contact of the solid with the redox electrode (Altmaier et al., 2010; Grenthe et al., 1992).

2.3. Degradation experiments

Before use, the UP2W material was washed with warm Milli-Q water at T = 65 °C, filtered and dried under ambient conditions. Two sets of batch experiments (see Table 1) were set up to investigate the hydrolytic degradation process, *i.e.*, leaching of organic degradation products of UP2W resin under conditions relevant in the context of L/ILW disposal.

The degradation experiments were set up in PTFE flasks and stirred magnetically (except the experiment at elevated temperature) with a PTFE-covered magnetic bar over the entire timeframe of the study. The batches were systematically monitored for pH, E_h (only in the presence of Fe(0)), non-purgeable organic carbon-content (NPOC) and after dilution with 2% HNO_3 for total calcium concentration via inductively coupled plasma – optical emission spectroscopy (ICP–OES, Optima 8300 DV, PerkinElmer). Separated aliquots of the different aqueous phases were analysed by ^1H, ^{13}C nuclear magnetic resonance spectroscopy (NMR) and size-exclusion/liquid chromatography – organic carbon detection – UV detection – organic nitrogen detection (LC-OCD-UVD-OND). Retrieved solid phases, *i.e.*, degraded UP2W material were characterized using X-ray photoelectron spectroscopy (XPS) and Fourier-transform infrared spectroscopy (FT-IR).

2.4. Aqueous phase characterization

2.4.1. Non-purgeable organic carbon (NPOC)

The leached organic content of the resin material was determined before and after filtration. Several tests performed in the present work identified the phase separation step as potential contributor to the measured dissolved organic content. In the course of these tests, numerous syringe filtration devices with different membrane materials (polystyrene-sulfone: 10 kDa MWCO, polycarbonate: 0.2 μm, cellulose acetate: 0.2 μm and PTFE: 0.1 or 0.45 μm) were used with varying volumes of leachates, and NPOC values were quantified before and after the filtration. These tests revealed that most of the filters initially release a given NPOC-content, which is generally washed out after two washing steps. PTFE-filters were identified as the most advantageous, *i.e.*, releasing a lower NPOC-content, whereas cellulose acetate filters resulted in significantly enhanced NPOC values even after the corresponding washing steps (with 100 and 1000 ppm C more for $Ca(OH)_2$-buffered and 0.1 M NaOH systems, respectively). This is probably the reason for the high TOC values reported by (Tasdigh, 2015), who used this type of filters for phase separation. PTFE filters (pore diameter = 0.1 or 0.45 μm GE Healthcare, Lifesciences, Whatman™) were washed three times with 1 cm^3 of background solutions identical to the target experiments to remove contributions of the remaining finishing products/impurities of the filters to the overall NPOC values. These background solutions were also stored in PTFE flasks in the glovebox just as the main experiments during the course of the study. In each sampling, aliquots of the supernatant solutions (5–10 cm^3) were centrifuged at 2876 *g* for 10 min to remove suspended particles. In the course of the subsequent filtration, first aliquots were directly disposed ensuring that the quantified NPOC levels correspond exclusively to the generated degradation products in solution. Background concentrations of NPOC were simultaneously quantified along with the samples on identically treated, filtered solutions and subtracted proportionally from the data obtained on the experiments. The effect of the filtration method on the NPOC concentrations was also taken into account by executing the exact same procedure on the background solutions and using the corresponding values for corrections.

After filtration, solutions were acidified with 2.0 M ultrapure HCl and transferred to glass vials to facilitate the removal of carbonate as well as to avoid the leaching of organics from the plastic vessel during storage. The quantification of NPOC values was performed with a Multi N/C 2100 S instrument (Analytik Jena) as calibrated with freshly prepared solutions of KH-phtalate applying high purity oxygen gas for degassing. Detection limit for direct NPOC measurements was approximately 0.1 ppm C in undiluted solutions. However, by taking into account the different background corrections on the NPOC levels and the effect of filtration, detection limits were raised for the real experiments to a level of 2–3 ppm C.

Table 1
Experimental conditions applied in the degradation batch samples containing UP2W.

#	degradation conditions	pH	Volume /dm^3	S:L ($Ca(OH)_2$) /g•dm^{-3}	S:L (UP2W) /g•dm^{-3}	S:L (Fe (0)) /g•dm^{-3}	T /°C
Long-term study (continuous stirring at 500 rpm):							
1	$Ca(OH)_2$-saturated sol.	12.5	1	50	50	–	(22 ± 2)
2	$Ca(OH)_2$-saturated sol., with Fe (0)	12.5	1	50	50	5	(22 ± 2)
3[a]	$Ca(OH)_2$-saturated sol. at elevated T	11.5	1	50	50	–	(80 ± 2)
4	Dilute NaOH solution	12.5	0.5	–	50	–	(22 ± 2)
5	0.10 M NaOH	~13	0.5	–	50	–	(22 ± 2)
6	1.00 M NaOH	~14	1	–	50	–	(22 ± 2)
Short-term study (continuous stirring until 130 days at 500 rpm, subsequently at 1400 rpm):							
7	$Ca(OH)_2$-saturated sol.	12.5	1	50	50	–	(22 ± 2)
8	$Ca(OH)_2$-saturated sol., with Fe (0)	12.5	1	50	50	5	(22 ± 2)
9	Dilute NaOH solution	12.5	0.25	–	50	–	(22 ± 2)
10	0.10 M NaOH	~13	1	–	50	–	(22 ± 2)

[a] Stirring was not possible for this sample, as it was placed in an oven to maintain T = (80 ± 2) °C.

2.4.2. ^{13}C nuclear magnetic resonance (NMR)

^{13}C NMR spectra of acidified or alkaline, filtered supernatant solutions (through pre-treated PTFE filters of 0.1 or 0.45 μm) in glass or PTFE liners were recorded at $T = 300$ K on a Bruker Avance III 400 spectrometer, operating at 100.63 MHz. The spectrometer was equipped with a z-gradient broadband observe probe optimized for x-magnetization detection (BBFOplus). Chemical shifts are provided in ppm and are referenced internally to tetramethylsilane, TMS (δ(TMS) = 0 ppm). ^{13}C NMR spectra were gained with proton decoupling and at an excitation angle of 30° with 8200 acquisitions for a better signal resolution.

2.4.3. Size exclusion/liquid chromatography – organic carbon detection – UV detection – organic nitrogen detection (LC-OCD-UVD-OND)

The liquid chromatographic system used within this study was developed by DOC-LABOR. Detailed information on the technique can be found elsewhere (Huber et al., 2011). The LC-OCD-UVD-OND system offers additional information compared to the conventional total organic carbon analysis by the coupling with a size exclusion chromatographic column (in the present work: TSK HW-50S, 250 mm × 20 mm, Tosoh Inc., Japan), which separates colloidal fractions before the analysis. It also includes a UV (UVD) and an organic nitrogen detector (OND) for the identification of any species absorbing in the UV region and for the quantification of organically bound nitrogen-content (after oxidation to nitrate). One part of the injected sample bypasses the chromatographic column for the determination of the NPOC and nitrogen content, while the other portion undergoes separation. According to the manufacturer, the calibration range of the HW-50S column is 20–0.5 kDa. In the present case, the system was calibrated against PAA or PSS standards in the ranges of 0.9–1020 kDa for molecular weight and 0.1–5 ppm for total organic carbon against freshly prepared solutions of KH-phtalate. In addition to these standards, titriplex (nitrilotriacetic acid), phthalic acid, glutaric acid, nitrate, sodium azide and ammonium were used as reference for lower molecular weight molecules. In the course of the three analyses campaigns, two different eluents were applied: 15 mM $NaHCO_3$ with pH ≈ 8.4 and a mixture of 7 mM Na_2HPO_4/15 mM KH_2PO_4 with pH ≈ 6.2–6.4. Note that the use of different eluents has an influence on the elution time of the standards used for calibration and has to be considered accordingly. The filtered aliquots (100 μL–2500 μL) of the supernatants (through pre-treated, 0.1 or 0.45 μm PTFE filters) from degradation experiments were first diluted with the eluents, and the resulting solutions were pH-adjusted whenever necessary. Selected measurements were conducted without previous pH-adjustment to avoid the interference of HNO_3 in the determination of the nitrate content in the samples. Additionally, filtered background solutions of identical compositions underwent analogous analyses to rule out the chromatographic signals related to impurities.

Table 2 summarizes the main experimental parameters considered for the characterization of the UP2W degradation leachates by LC-OCD-UVD-OND.

2.5. Solid phase characterization

Degraded UP2W solid phases were retrieved in small fractions (200–500 mg) from the batch experiments as suspensions, and centrifuged at 2876 *g* for the removal of the supernatant solution. The separated solids were then washed rapidly twice with 5 mL of 2 M Ultrapur HCl and twice with MilliQ water. In between, centrifugation steps ensured phase separation of the re-suspended polymer particles from the matrices. The whole procedure was performed also on the original UP2W material to monitor the invasiveness of the sample preparation method. The solids were finally dried under Ar atmosphere for several days and characterized by XPS and FT-IR.

2.5.1. Fourier transform - infra red spectroscopy (FT- IR)

The functional groups of the UP2W material before and after degradation were probed by means of FT-IR using an IFS44 Bruker Optics equipment with attenuated total reflectance (ATR) accessory and deuterated triglycine sulfate (DTGS) detector. Before measurement, the equipment was cooled down with liquid nitrogen ($T = -195.79$ °C). For each sample, 64 scans were collected in the range of 4000–400 cm^{-1}. The solid samples were pressed in a cell with the help of a sapphire punch.

2.5.2. X-ray photoelectron spectroscopy (XPS)

XPS measurements were performed with an XPS system PHI 5000 VersaProbe II (ULVAC-PHI Inc.) equipped with a scanning microprobe X-ray source (monochromatic Al K_α, $h\nu = 1486.7$ eV). An electron flood gun generating low energy electrons (1.1 eV) and low energy argon ions (8 eV) by a floating ion gun were applied for charge compensation at isolating samples (dual beam technique), respectively. Survey scans were recorded with an X-ray source power of 33 W, X-ray spot size diameter 160 μm, and pass energy of the analyser of 187.85 eV. Narrow scans of the elemental lines were recorded at 23.5 eV pass energy, which yields an energy resolution of 0.69 eV FWHM at the Ag $3d_{5/2}$ elemental line of pure silver. Calibration of the binding energy scale of the spectrometer was performed using well-established binding energies of elemental lines of pure metals (monochromatic Al K_α: Cu $2p_{3/2}$ at 932.62 eV, Au $4f_{7/2}$ at 83.96 eV) (Seah et al., 1998). Error of binding energies of elemental lines is estimated to ±0.2 eV. N 1s at 399.57 eV is used as charge reference for acrylonitrile sample (Beamson and Briggs, 2012) and C 1s (C_xH_y) at 284.8 eV for degraded samples.

Table 2
Samples considered for the characterization of the UP2W degradation leachates, and main experimental conditions for LC-OCD-UVD-OND.

Degradation time [days]	Degradation solutions	Eluent	Figure number
595 (only for test experiments)	pH = 12.5, NaOH, with pH regularly adjusted 0.1 M NaOH (no pH adjustment) 1.0 M NaOH (no pH adjustments)	15 mM $NaHCO_3$ pH ≈ 8.4 (no addition of HNO_3)	
701	pH = 12.5, buffered by $Ca(OH)_2$, $T = 22$ °C pH = 12.5, NaOH, with pH regularly adjusted 0.1 M NaOH (no pH adjustment) 1.0 M NaOH (no pH adjustments)	7 mM Na_2HPO_4/15 mM KH_2PO_4 pH ≈ 6.2–6.4 (+HNO_3 before measurements)	Fig. 6a Fig. 6d Fig. 6e Fig. 6b
1200	pH = 12.5, buffered by $Ca(OH)_2$, $T = 22$ °C pH = 12.5, buffered by $Ca(OH)_2$, with Fe (0) powder, $T = 22$ °C	15 mM $NaHCO_3$ pH ≈ 8.4 (+HNO_3 before measurements)	Fig. 6b
1838	pH = 12.5, buffered by $Ca(OH)_2$, $T = 22$ °C pH = 12.5, buffered by $Ca(OH)_2$, with Fe (0) powder, $T = 22$ °C	15 mM $NaHCO_3$ pH ≈ 8.4 (+HNO_3 before measurements)	Fig. 6c
1838	pH = 12.5, buffered by $Ca(OH)_2$, $T = 22$ °C pH = 12.5, buffered by $Ca(OH)_2$, with Fe (0) powder, $T = 22$ °C	15 mM $NaHCO_3$ pH ≈ 8.4 (no addition of HNO_3)	Fig. 7

Atomic concentrations were calculated by areas of elemental lines of survey spectra after subtraction of a local Shirley background and taking into account sensitivity factors and asymmetry parameters of elemental lines, and transmission function of the analyser. Relative error of atomic concentrations is within ± (10–20)%. Curve fits to narrow scans of elemental lines were performed by Gaussian-Lorentzian sum functions after Shirley background subtraction. Molar concentrations of elemental species were calculated by atomic concentrations and curve fit results. Data analysis was performed using ULVAC-PHI MultiPak program, version 9.9.

3. Results and discussion

3.1. Aqueous phase characterization

3.1.1. Evolution of leached organic content

Fig. 2 shows the time evolution of the dissolved organic carbon in the $Ca(OH)_2$-buffered degradation experiments (with and without Fe (0), at $T = 22$ and 80 °C) for contact times of up to 1838 days, *i.e.*, *ca.* 5 years. Data gathered for NaOH systems are displayed in Fig. 3.

NPOC values determined in $Ca(OH)_2$-buffered systems remain very low (<10 ppm) for up to ~ 600 days (Fig. 2). These values are in line with the previous UP2W degradation study conducted by (Duro et al., 2012) in analogous $Ca(OH)_2$-buffered systems (see also Fig. 4). Beyond ~700 days, NPOC values in $Ca(OH)_2$-buffered systems at $T = 22$ °C show a significant enhancement, reaching ~ 30 ppm C (absence of Fe (0)) and ~50 ppm C (presence of Fe (0)) at a contact time of ~1800 days (Fig. 2). Differences observed between $Ca(OH)_2$-buffered systems in the absence and presence of Fe (0) may be caused by the impact of the redox conditions on the degradation mechanism, although the uncertainties associated to the NPOC measurements do not allow to draw definitive conclusions in this respect.

The relatively low NPOC values (~10 ppm after 1239 days) determined for the $Ca(OH)_2$-buffered sample equilibrated at $T = 80$ °C could be attributed to two main factors: (i) the lack of stirring for this sample, which was stored in an oven inside the glovebox, and (ii) the decreased solubility product of $Ca(OH)_2$ at elevated temperature, which results in lower concentrations of Ca^{2+} and OH^- ions. Option (i) might be disregarded on the basis of degradation experiments performed at increased stirring velocity (1400 rpm instead of 500 rpm), which did not show evidence of an enhanced UP2W degradation/dissolution rate in Ca $(OH)_2$-buffered systems at $T = 22$ °C for a time period of ~170 days (see Fig. 2).

The degradation behavior of UP2W at $T = 80$ °C observed in the current work is apparently in disagreement with previous studies, which reported an enhancement of the degradation/dissolution rate with temperature: ~250 ppm after 3 months at T = 60 °C (Tasdigh, 2015); 1400 ppm and 1000 ppm, after 1.5 months at T = 60 °C with $[Ca]_{tot}$ = 0.01 M and 3 months without Ca, respectively (Duro et al., 2012). A

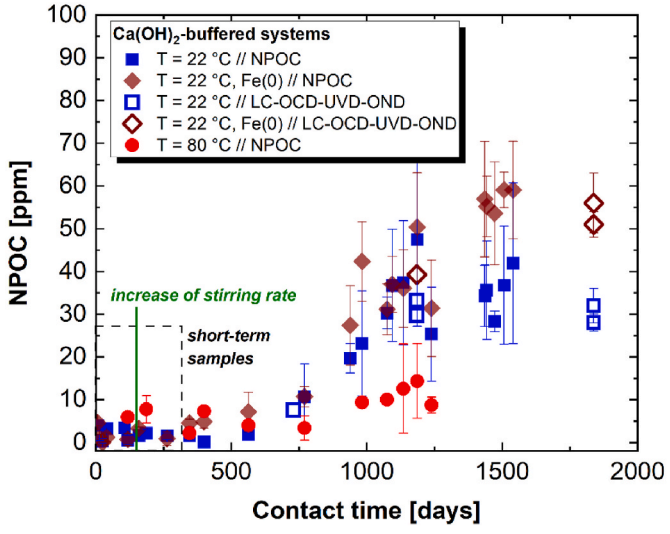

Fig. 2. Evolution of the NPOC during the UP2W degradation experiments in Ca $(OH)_2$-buffered systems (with and without Fe (0), at T = 22 and 80 °C). Empty symbols correspond to NPOC values determined by means of LC-OCD-UVD-OND. Short-term samples were prepared to assess the effect of the stirring rate, i.e. at 500 rpm for 130 days, subsequently at 1400 rpm for up to 300 days. Uncertainties calculated as three times the standard deviation of 3–5 replicates. ICP-OES measurements confirmed [Ca] consistent with solubility of $Ca(OH)_2$ at pH ≈ 12.5.

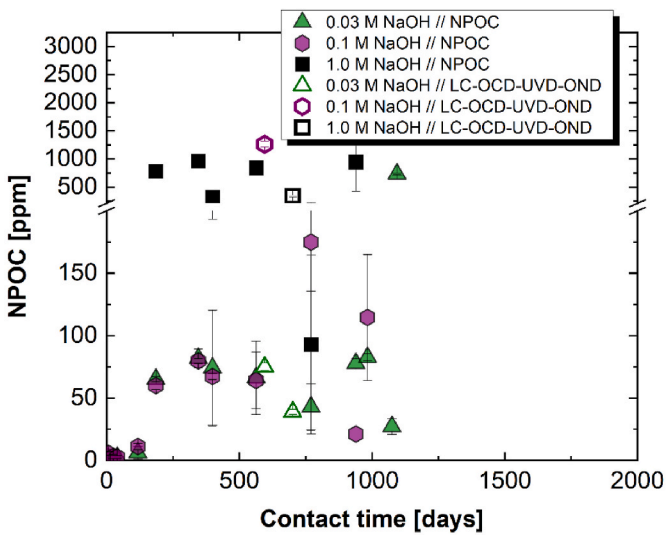

Fig. 3. Evolution of the NPOC during the UP2W degradation experiments in NaOH systems at T = 22 °C. Empty symbols correspond to NPOC values determined by means of LC-OCD-UVD-OND. Uncertainties calculated as three times the standard deviation of 3–5 replicates.

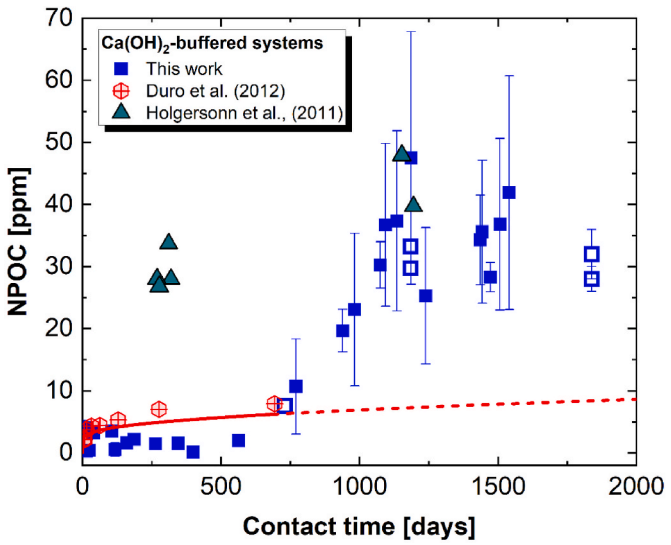

Fig. 4. Comparison of the NPOC values determined in this work for the degradation of UP2W in $Ca(OH)_2$-buffered systems at T = 22 °C and data reported under analogous conditions by Duro et al. and Holgersson et al. Empty symbols correspond to NPOC values determined in this work by means of LC-OCD-UVD-OND. Uncertainties calculated as three times the standard deviation of 3–5 replicates. Red line illustrates the empirical kinetic model reported in (Duro et al., 2012).

closer look to both publications reveals that (Tasdigh, 2015) experienced the total dissolution of the added solid $Ca(OH)_2$ and a pH-drop (reaching ~ 9.3 at $t = 240$ days) in the samples at $T = 60$ °C, whilst for the same temperature (Duro et al., 2012) used a Ca concentration insufficient to reach a near-stoichiometric ratio with respect to the available functional groups/monomer units considering the S:L ratio used in the experiments.

Compared to $Ca(OH)_2$ systems, significantly higher NPOC values were systematically quantified in NaOH systems, following the order 0.03 M NaOH (pH = 12.5) < 0.1 M NaOH ≪ 1.0 M NaOH. This observation underlines the key role of hydroxide in the degradation mechanism of PAN (Litmanovich and Platé, 2000). The comparison of NaOH and $Ca(OH)_2$ systems shows as well that the increase in NPOC takes place after an induction period of ~100 and ~500 days, respectively. These results underpin that the presence of Ca contributes to the stabilization of intermediates, which possibly are less prone to chain scission and subsequent cross-linking. Shortly after the start of the degradation experiments in NaOH systems, the solid phase turned yellowish, then red, whilst the solution remained yellow throughout the entire time, in good agreement with observations reported in the literature (Bashir et al., 1991). The viscosity of the solutions in the degradation experiments in NaOH increased rapidly, also following the trend described in (Bashir et al., 1991). Hence, after 400 days of contact time, degradation experiments in 1.0 M NaOH developed a gel-like texture, which prevented phase separation through the original 0.1 μm filters and required the use of filters with larger cut-off, *i.e.*, 0.45 μm. After *ca.* 1000 days, filtration of this degradation solution was not anymore possible. The observations in NaOH systems hint towards a fast degradation and fragmentation, followed by cross-linking of the fragments in solution. Note however that the evolution of the NPOC values in these systems must be carefully used to evaluate the degradation kinetics, due to the difficulties for the accurate quantification of the truly dissolved organic content in solution.

The comparison of the degradation experiments at pH ≈ 12.5 in NaOH- (with pH-readjustments) and $Ca(OH)_2$-buffered samples at $T = 22$ °C clearly shows that the presence of Ca (with constant aqueous concentration as buffered by $Ca(OH)_2$) has a strong hindering effect on the scission and release of soluble UP2W fragments. However, also Ca $(OH)_2$-buffered systems experience an increase in the concentration of dissolved species at $t > 700$ days, as also confirmed by LC-OCD-UVD-OND (see Section 3.1.3).

Fig. 4 shows the comparison of the NPOC values determined in this work for $Ca(OH)_2$-buffered systems at $T = 22$ °C with analogous data reported in (Duro et al., 2012; Holgersson et al., 2011). Note that data reported by (Holgersson et al., 2011) for the two first samplings of batches 1 and 2 are not included in the figure due to the problems identified by the authors in the quantification of TOC. Fig. 4 shows also the empirical kinetic model derived by (Duro et al., 2012) based on their degradation data up to a contact time of 694 days. The very high NPOC values reported by (Tasdigh, 2015) are disregarded in this comparison due to the problems identified with the phase separation method used by the author, which relied on cellulose acetate filters. As discussed above, this type of filters was shown to leach very high organic content even after several washing steps, to which we attribute the significantly higher TOC values reported by the author.

NPOC data reported by (Duro et al., 2012) for contact times up to 694 days qualitatively agree with our results up to contact times of ~600 days, reflecting rather low NPOC values (<10 ppm) and slow degradation/dissolution kinetics. The corresponding kinetic law derived by (Duro et al., 2012) explains well NPOC data up to these contact times, but fails to reproduce the observations obtained in the present work at $t \geq 800$ days, which show a significantly faster increase of the NPOC values up to contact times of ~1800 days. The latter values are consistent with the long-term degradation results by (Holgersson et al., 2011). However, no evident explanation can be provided for the discrepancies with data reported by (Holgersson et al., 2011) at $t < 500$ days.

In the modelling of their experimental data, (Duro et al., 2012) observed a logarithmic dependence of TOC with time, which was attributed to several parallel and competitive processes taking place in the system. TOC is thus an overall measurement involving all organic degradation products, which cannot respond to a unique kinetic reaction. Most of the degradation studies published to date have focussed on the description of the evolution of the solid PAN material (Bajaj et al., 1985; Litmanovich and Platé, 2000). This involves a number of steps in the solid phase, *e.g.*, the formation of intermediate amides and amidines, the release of ammonia and the ultimate formation of carboxylate groups. Several of these steps are triggered by the nucleophilic attack of a hydroxide ion to a nitrile or carbonyl group, which underpins that the hydrolysis rate is increased at higher pH values. However, beyond these reactions driven in the bulk polymer, scission as well as cross-linking reactions taking place within the degradation leachates are key to understand the evolution of the dissolved organic content in the course of UP2W degradation. Moreover, the relevant differences observed between NaOH- and $Ca(OH)_2$-buffered systems with the same pH highlight also the key role of the Ca^{2+}-ion in the evolution of the degradation process.

3.1.2. Solution ^{13}C NMR of UP2W degradation leachates

A number of ^{13}C NMR studies previously focused on the characterization of the bulk fraction of hydrolyzed PAN (Bajaj and Kumari, 1988; Dyatlov et al., 2012; Ermakov et al., 2000; Jin et al., 2017). However, to our knowledge, this work is the first attempt to apply this technique for the characterization of the degradation leachates generated by the alkaline hydrolysis of PAN as the main component of UP2W.

Only the degradation leachates generated in 1.0 M NaOH solutions attained sufficiently high concentrations of dissolved organic carbon (quantified as NPOC, see Figs. 2 and 3) as to be characterized by ^{13}C NMR. For this degradation matrix solution, Fig. 5 displays the proton-decoupled ^{13}C NMR spectra collected for aliquots of UP2W leachates after contact times of 425 (Fig. 5a) and 970 (Fig. 5b) days. Accounting for the presence of the broad signal in Fig. 5a corresponding to the PTFE sample holder, spectra collected at 970 days were taken instead in standard glass-tubes with neutralized aliquots..

Fig. 5 shows similar ^{13}C NMR spectra at $t = 425$ and 970 days. Consistent signals are observed at $\delta(^{13}C) \approx 36$ and ~45 ppm, which can be assigned to methylene and methine carbon resonances, respectively (Ermakov et al., 2000; Truong et al., 1986a, 1986b). We note the absence of the signal at ~120 ppm corresponding to the cyano carbon (Choi et al., 2011; Wang et al., 2014), which underpins that in 1.0 M NaOH the transformation of the nitrile group into amide and carboxylic groups in the degradation leachates is complete within the considered timeframe (≥425 days). Following the peak assignment by (Truong et al., 1986a), carbonyl resonance peaks can be separated into two triads, one centered at around 181 ppm, representing amides (A) with neighboring amide and carboxylate (C) groups (AAA, CAA, CAC), and the other peak located at around 184 ppm, showcasing the presence of the analogous triads for carboxylate groups (CCC, ACC, ACA). Details on the peak positions are provided in Table 3. Compared to the 425 days leachate (Fig. 5a), the spectra of the more degraded fragments after 970 days (Fig. 5b) displays a proportionally higher relative-ratio of the low-field signals within the triads (from the amide signals: CAA (peak 5) and CAC (peak 4) and from the carboxylate ones, the CCA (peak 2) and CCC (peak 1)). This trend reflects that similar transformations take place in solution and in the bulk of the polymer. The signals of the methine carbon appear to be split into two groups and are located low field to the methylene carbon signals, displaying also the extensive hydrolysis of the original nitrile functional groups. Methine-carbons with amide groups are high-field to the carboxylic acid-connected ones, and the more amide groups are on the neighboring methine-carbon atoms, the higher the field is, where their signals appear. As for the carboxylic acid group-connected methine resonances, the methine-carbon resonance of 7, 8, 9, as indicated in Fig. 5b correspond to the alpha-carbon atoms next

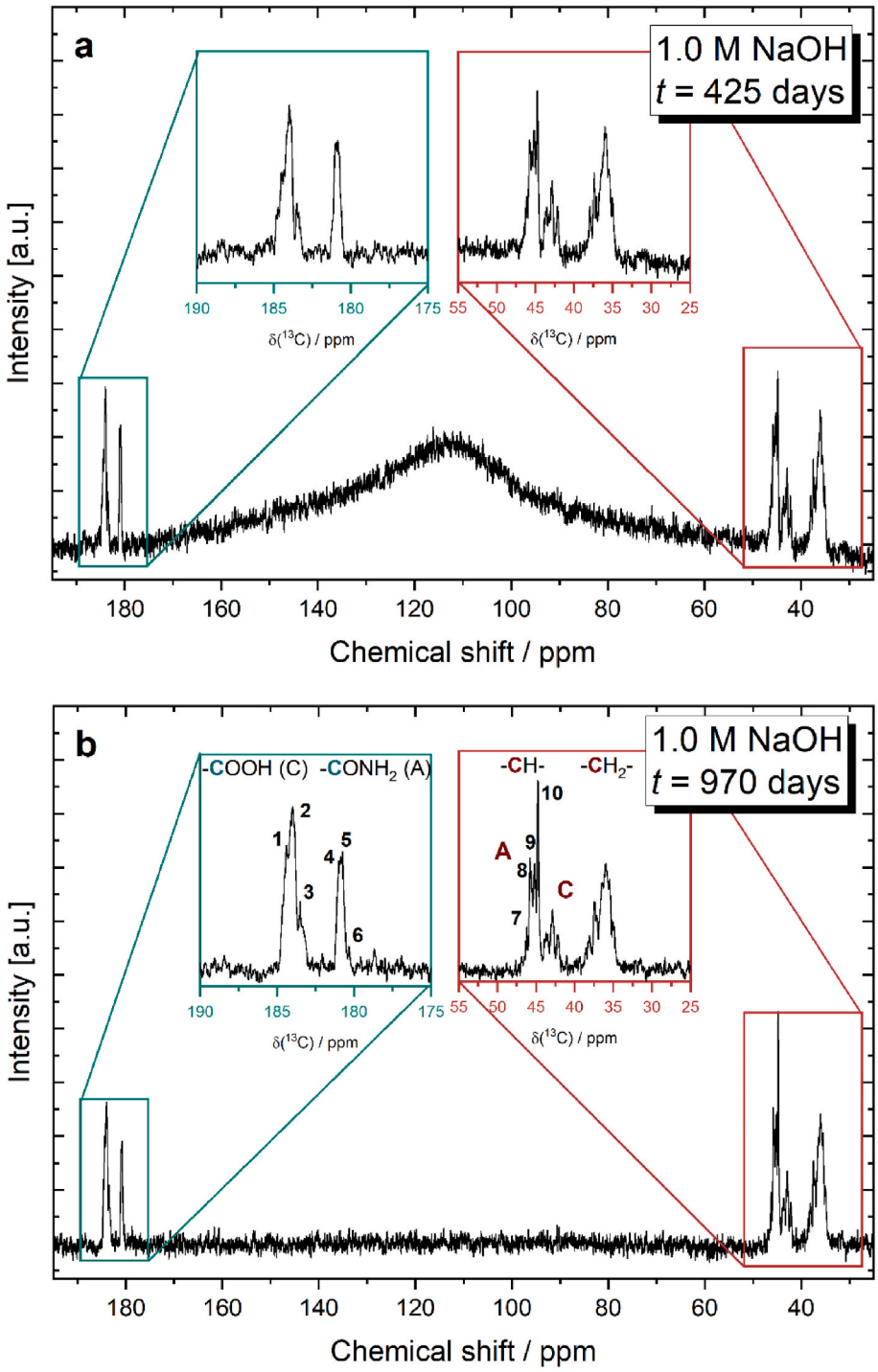

Fig. 5. Proton-decoupled ^{13}C NMR spectra of filtered degradation leachates retrieved from the 1.0 M NaOH experiment at 425 (**a,** in PTFE sample holder, alkaline) and 970 days (**b,** in glass tube, neutralized) of contact time.

to carboxylate groups with one or two neighboring amide groups (Truong et al., 1986b). As expected, with the propagation of the hydrolysis, the relative ratio of the latter peaks to the amide group-centered methine carbon signals increased over time. On the other hand, the resonance at approximately 44.9 ppm chemical shift (peak 10 in Fig. 5b), as indicative of the presence of hetero- and syndiotactic CCC triads (repeating units have alternating stereochemical configurations, suffered a more significant increase, disproportionate to the intensities of the other carboxylic acid-related methine carbon peaks. The latter observation points towards the gradual accumulation of carboxylic acid groups on the dissolved polymeric chains, again showing a very similar transformation pattern to the one seen in the solid polymer.

3.1.3. LC-OCD-UVD-OND of UP2W degradation leachates

Fig. 6 shows the OC-chromatograms collected after the injection of the eluates of the UP2W degradation leachates (NaOH- and $Ca(OH)_2$-buffered systems) at degradation times of 701 and 1200 days, whereas Figs. SI–1 in the Supporting Information presents the corresponding OC-, UV- and ON-chromatograms. Fig. 7 shows the OC-, UV- and ON-chromatograms obtained at $t = 1838$ days for the analysis of $Ca(OH)_2$-buffered samples (without acidification). At $t \geq 1200$ days, samples in

Table 3
Chemical monomer triad assignments for ^{13}C NMR spectra of amide (A) and carboxylate (C) carbonyl resonances for polyacrylonitrile hydrolyzed in 1.0 M NaOH, based on the work by Truong et al. (1986a). [Comment to editors: in the editing of this manuscript, please keep Table 3 directly below Fig. 5, as information provided in them are very much interconnected].

Functional group and peak number	Chemical shift/ppm	Assignment
Carbonyl resonances		
carboxylic acid – 1.	184.5	C–C–C
carboxylic acid – 2.	184.0	C–C-A
carboxylic acid – 3.	183.5	A-C-A
amide – 4.	181.5	C-A-C
amide – 5.	181.0	C-A-A
amide – 6.	180.5	A-A-A

NaOH systems could not be characterized due to the significantly enhanced viscosity of the degradation leachates. NPOC values determined for the degradation leachates at t = 701, 1200 and 1838 days integrating the peak area in the OC spectra are in line with independent NPOC measurements discussed in Section 3.1.1 (see empty symbols in Figs. 2–4).

Molecular weights estimated from the retention times (based on calibration with PSS) of the main peak assigned to the UP2W degradation leachates obtained after degradation times of 701, 1200 and 1838 days are summarized in Table 4. These are calculated as interpolated values using the corresponding calibration curves according to the eluent used. All investigated systems are characterized by a complex distribution of size fractions, although in most cases the largest size fraction represents the main OC-contribution. Degradation leachates obtained after 701 days in NaOH systems are characterized by significantly large molecular weights, *i.e.* > 33 kDa. These values translate in *ca.* 460 equivalent monomer units, calculated as units of polyacrylic acid. In contrast to this, manifestly smaller fragments are observed for the degradation leachates obtained at 701 days in $Ca(OH)_2$ systems, *i.e.,* from *ca.* 0.9 kDa (*ca.* 12 equivalent monomer units) to *ca.* 3 kDa (*ca.* 40 equivalent monomer units), with a significant fraction of low molecular weight (LMW) organics eluting at retention times similar to glutaric acid. The degradation leachates in $Ca(OH)_2$ systems collected at t = 1200 and 1838 days show an evident and systematic increase in the molecular weight of the organic fragments in solution, with a main fraction of the fragments attaining ≥15.8 kDa (*ca.* 220 equivalent monomer units) at t = 1838 days, both in the absence and presence of Fe (0). This observation supports that cross-linking of dissolved fragments is also a relevant process in Ca $(OH)_2$-buffered systems, in spite of the significantly lower dissolved organic content. A shoulder of the main OC-peak appears at $t \approx$ 30–32 min (1.7–3.4 kDa), which is however mainly visible for the $Ca(OH)_2$-buffered system containing Fe (0). A minor fraction of the degradation leachates is eluted at $t \approx$ 38 min, which is in line with the presence of small molecular weight organic ligands, *e.g.*, as the phthalic or glutaric acids used as references.

Scission and cross-linking of PAN were previously investigated by (Bashir et al., 1991). Based on their own experimental evidences and previous postulations in the literature (Schurz, 1958; Zahn and Schäfer, 1959), the authors claimed the susceptibility of the methine proton to abstraction by strong base as trigger for both scission (1) and cross-linking (2) reactions.

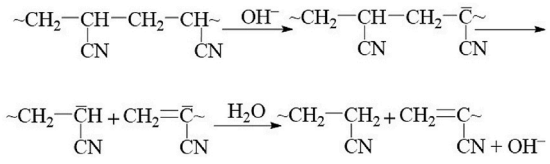

(1)

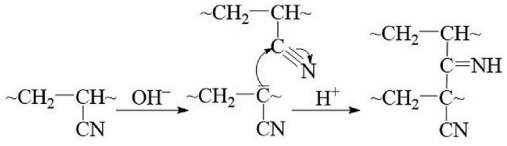

(2)

Schemes (1) and (2) support that both scission and cross-linking reactions are favored at increasing hydroxide concentrations, which is in line with NPOC and LC-OCD-UVD-OND observations in this work for the degradation of UP2W in NaOH systems. Our results evidence also the key role of Ca in decreasing the scission rate, which we interpret as the impact of Ca^{2+} in the methine proton abstraction, possibly caused by the complexation of the calcium ion with amide and carboxylate groups in the hydrolyzed PAN and the consequent impact on electron-pair distribution and resonances.

The clear correlation between the OC peak corresponding to the UP2W degradation products and the UV signal at λ = 225 nm is supporting the presence of carboxylate groups at ~701–1838 days, in NaOH- and Ca $(OH)_2$-buffered systems. For the same OC peak, the ON detector confirms the presence of nitrogen groups at the two degradation times investigated. This observation supports that the transformation of the nitrile groups of PAN into carboxylates is not complete even after 1838 days. The very last prevalent signal observed in all ON chromatograms ($t \approx$ 120–150 min) can be assigned to the ammonium ion, which is expected in solution as end-product in the alkaline hydrolysis of the nitrile groups of PAN.

The evaluation of the C/N ratio in the degradation leachates can be done based on the OC and ON signals in the region 20–40 min. A clear

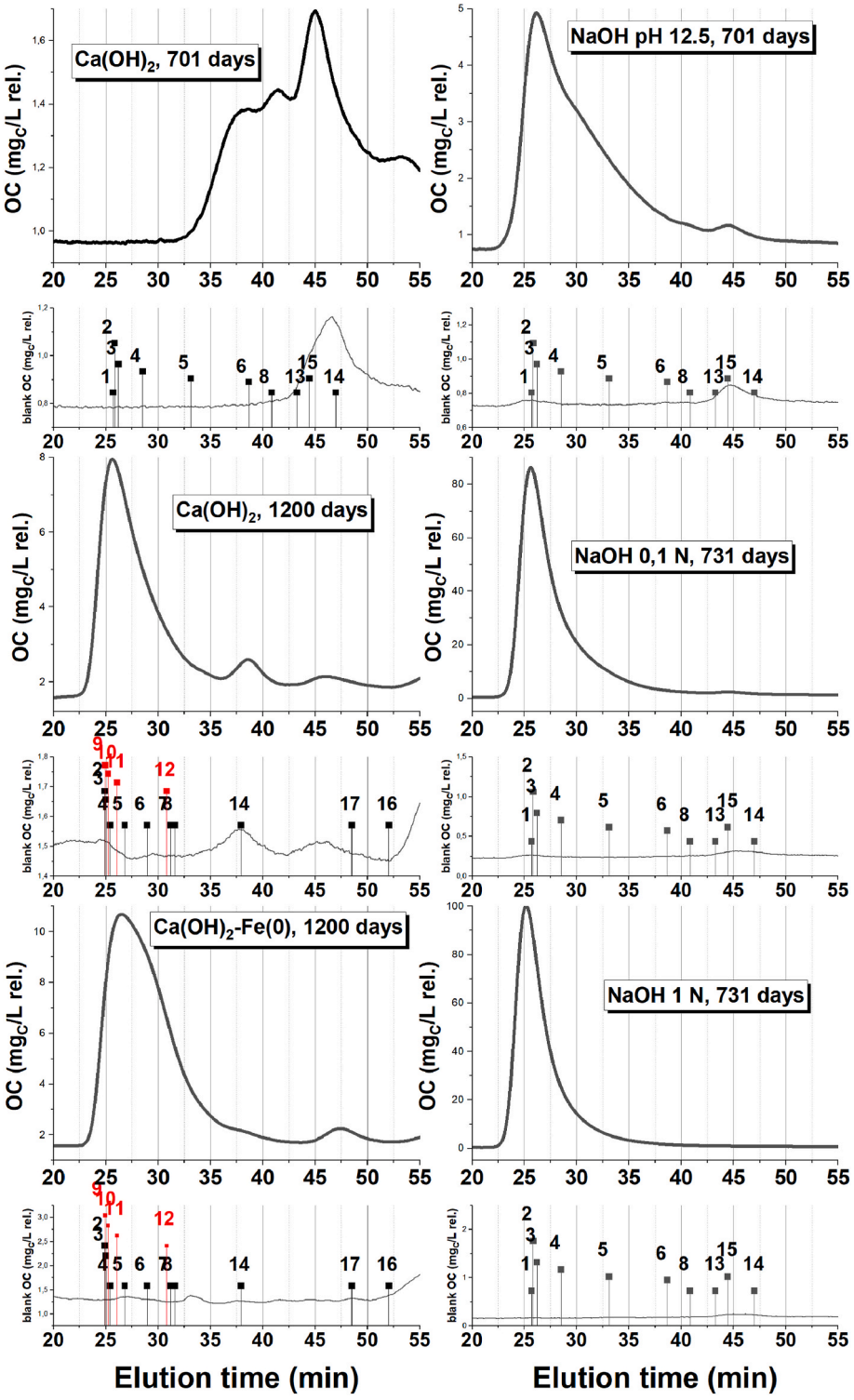

Fig. 6. OC-chromatograms obtained after chromatographic separation of the UP2W degradation leachates collected at contact times of 701 or 731 and 1200 days. Figures correspond to degradation leachates obtained in $Ca(OH)_2$- (left) and NaOH- (right) systems. Underneath graphs correspond to the OC-chromatogram of blank samples. Numbered lines indicate the elution times of the different references *i.e.* PSS (in black), PAA (in red), as well as small molecular weight ligands and molecules (in black): 1.PSS 1020 kDa; 2: PSS 65.4 kDa; 3: PSS 33.5 kDa; 4: PSS 15.8 kDa; 5:PSS 6.43 kDa; 6: PSS 3.42 kDa, 7: PSS 1.67 kDa, 8: PSS 0.891 kDa; 9: PAA 62.8 kDa, 10: PAA 16 kDa; 11: PAA 4.1 kDa, 12: PAA 1.25 kDa; 13: Titriplex; 14: Phtalate (~0.163 kDa); 15: Glutaric acid; 16: Nitrate (~0.0615 kDa); 17: Sodium azide (~0.0645 kDa); 18: Ammonium. Suspensions were acidified with HNO3, which is also reflected in the corresponding UV- and ON-chromatograms (see Supporting Information).

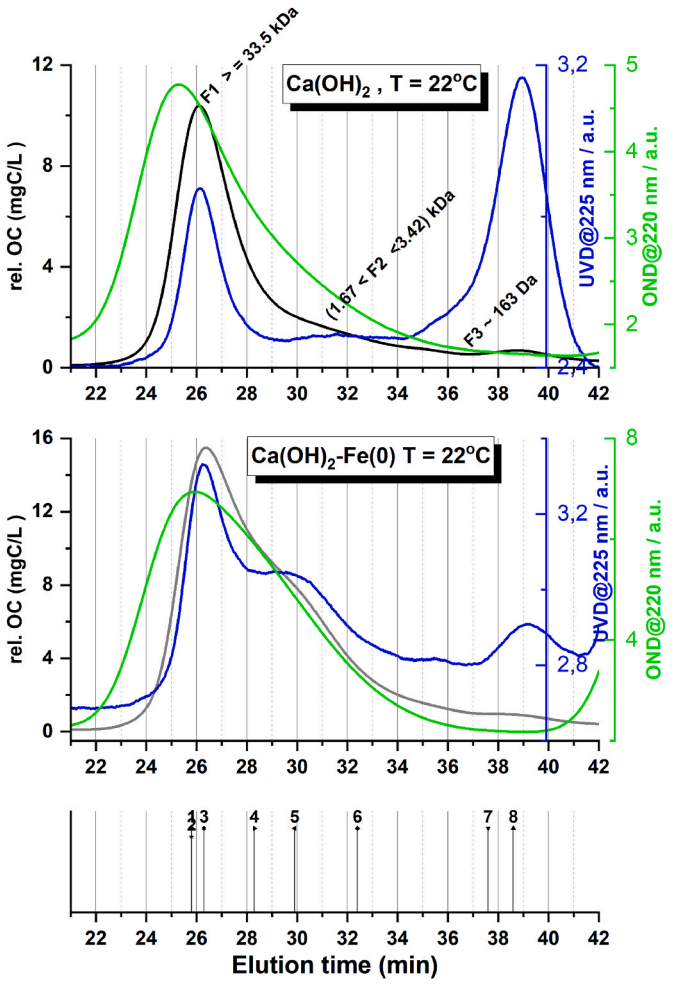

Fig. 7. OC- (black), UV- (blue) and ON-chromatograms (green) obtained after chromatographic separation of the UP2W degradation leachates collected at a contact time of 1838 days. Figures correspond to degradation leachates obtained in $Ca(OH)_2$-buffered systems in the absence and presence of Fe (0). Numbered lines correspond to the elution times of the different references i.e. PSS as well as small molecular weight ligands and molecules: 1.PSS 65.4 kDa; 2: PSS 33.5 kDa; 3: PSS 15.8 kDa; 4: PSS 6.43 kDa; 5: PSS 3.42 kDa, 6: PSS 1.67 kDa, 7: PSS 0.891 kDa; 8: Phtalate (~0.163 kDa); 9: Sodium azide (~0.0645 kDa); 10: Nitrate (0.0615 kDa).

trend can be observed for data collected in NaOH systems at $t = 700$ days, with C/N = (2.2 ± 0.2) for the system at pH = 12.5, C/N = (12 ± 1) for the system in 0.1 M NaOH and C/N = (25 ± 9) for the system in 1.0 M NaOH. Similar trends are observed for $Ca(OH)_2$ systems in the absence and presence of Fe (0), with C/N = (4 ± 1) at $t = 700$ days, and increased but constant C/N ratios between 1200 and 1838 days, *i.e.*, C/N ~ 11–14. These observations reflect a substantial but incomplete hydrolysis of the nitrile and/or amide groups in all investigated degradation leachates.

3.2. Solid phase characterization

3.2.1. FT-IR

Fig. 8 shows the FT-IR spectra collected for UP2W solid phases retrieved from the NaOH-systems after a contact time of 740 days. Besides the features of the original PAN material, the FT-IR spectra of the NaOH-degraded PAN fibres clearly show the presence of additional functional groups, suggesting the gradual transformation of the nitrile groups. Assignment of the characteristic IR signals corresponding to the untreated PAN fibre is as follows (Bashir et al., 1991; Duro et al., 2012; Dyatlov et al., 2012; Lee et al., 2017; Liang and Krimm, 1958; Pérez-Alvarez et al., 2019): 1454 cm^{-1}: bending mode of $–CH_2$ on the backbone of the polymer, 2239 cm^{-1}: C≡N stretching mode. The region of ~700–1400 cm^{-1} contains the various bending, wagging and twisting modes of C–H and C–C bonds, often referred to as the structural fingerprint of a polymer, highly sensitive to modifications. Notable is the appearance of the C≡N stretching mode as a singlet indicating that the polymer is not syndiotactic (repeating units with alternate stereochemical configurations), but rather close to being isotactic (repeating units with same stereochemical configuration). Since the spectral accumulation was performed under ambient conditions, the typical doublet of carbon dioxide is also visible at around 2300 cm^{-1}. Additionally, in the region of 1600–1800 cm^{-1} the broader peaks with relatively low intensities correspond to impurities in the original material.

After 740 days of degradation in NaOH media, the IR spectra of the polymer shows a clear decrease in the C≡N stretching signal at 2239 cm^{-1}, thus confirming the progress of PAN hydrolysis. The decrease of this feature is correlated with the hydroxide concentration, *i.e.*, the extent of hydrolysis increases following the sequence 0.03 M (pH = 12.5, readjusted) < 0.1 M < 1.0 M NaOH, in line with the results obtained for the characterization of the degradation leachates. Moreover, two new peaks arise at ~1565 and ~1666 cm^{-1} in all samples equilibrated in NaOH media (Fig. 8). These signals are related to the bending mode of N–H bonds (typical for amines and amides) in carboxamide and the stretching mode of carbonyl group (C=O) in carboxamide and carboxyl

Table 4
Retention times (from OC-chromatograms) and estimated molecular weights of the UP2W degradation leachates obtained after degradation times of 701, 1200 and 1838 days. Note that slight variation in the retention times of the PSS references arise between LC-OCD-UVD-OND measurements at $t = 1200$ and 1838 days, although the same eluent was used, *i.e.*, $NaHCO_3$.

	Degradation time: 701 days Eluent: Na_2HPO_4/KH_2PO_4		Degradation time: 1200 days Eluent: $NaHCO_3$		Degradation time: 1838 days Eluent: $NaHCO_3$	
Sample	Retention time [min][a]	Molecular weight [kDa]	Retention time [min][a]	Molecular weight [kDa]	Retention time [min][a]	Molecular weight [kDa]
$Ca(OH)_2$	38.1, 41, 45	~3.4, 0.9, LMW	25.6, 38, 47	~16, LMW, very LMW	~26, 31 (shoulder), 35, 38	≥15.8, 1.7–3.4, 0.9–1.6, LMW
$Ca(OH)_2$ + Fe(0)			26.5, 31 (shoulder), 38 (shoulder), 47	6.4–15.8, 0.9–1.6, LMW, very LMW	26.4, 31	≥15.8, 1.7–3.4
NaOH, pH = 12.5	26.2, 29–40, 45	34–65, 3.4–15.8, LMW	–	–	–	–
0.1 NaOH	25.6, 31	>65.4[b], ~6.4	–	–	–	–
1.0 NaOH	25.6	>65.4[b]	–	–	–	–

[a] Retention times based on the OCD signal;
[b] Retention times at the exclusion limit of the calibration curves. Molecular weight could not be quantified.

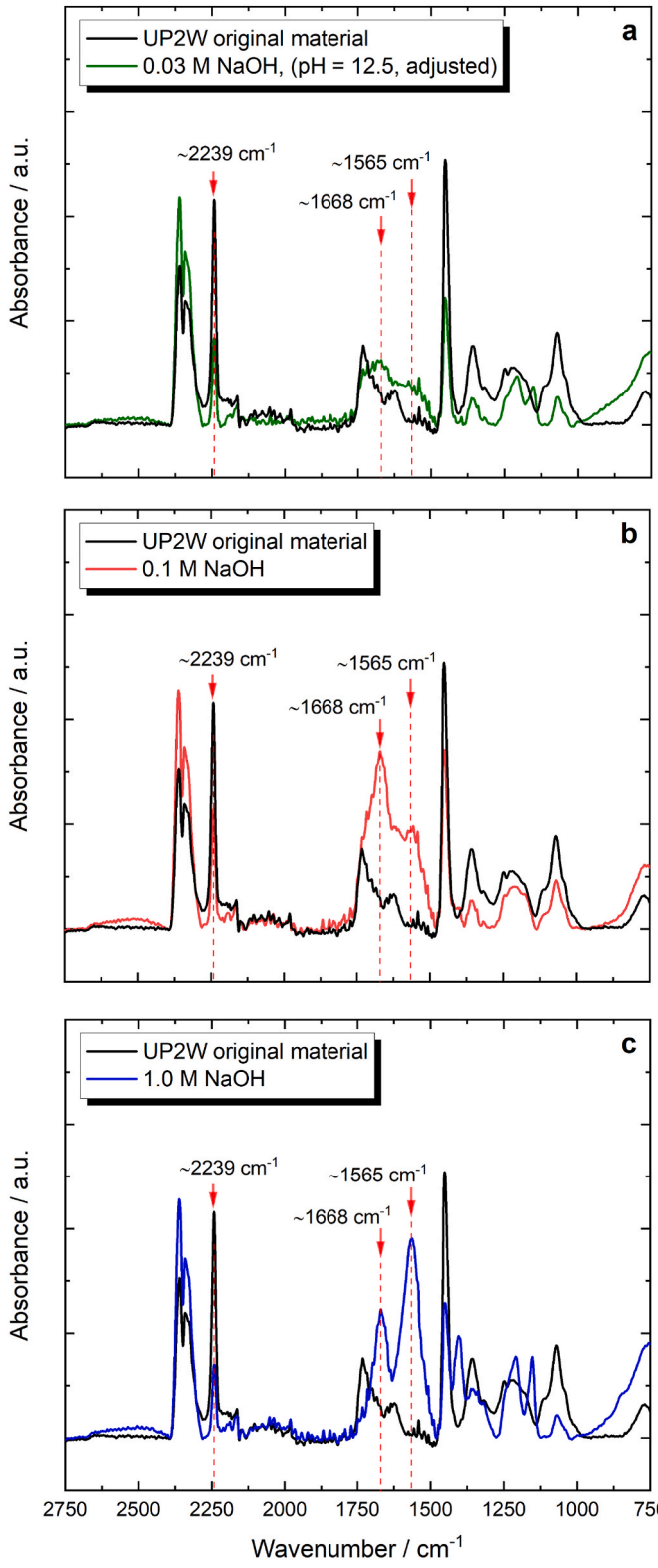

Fig. 8. Solid state FT-IR spectra of UP2W material degraded for 740 days in NaOH systems at T = 22 °C: **(a)** 0.03 M (pH = 12.5, re-adjusted); **(b)** 0.1 M NaOH; **(c)** 1.0 M NaOH. Black line in all figures corresponds to the FT-IR spectrum of the original UP2W material.

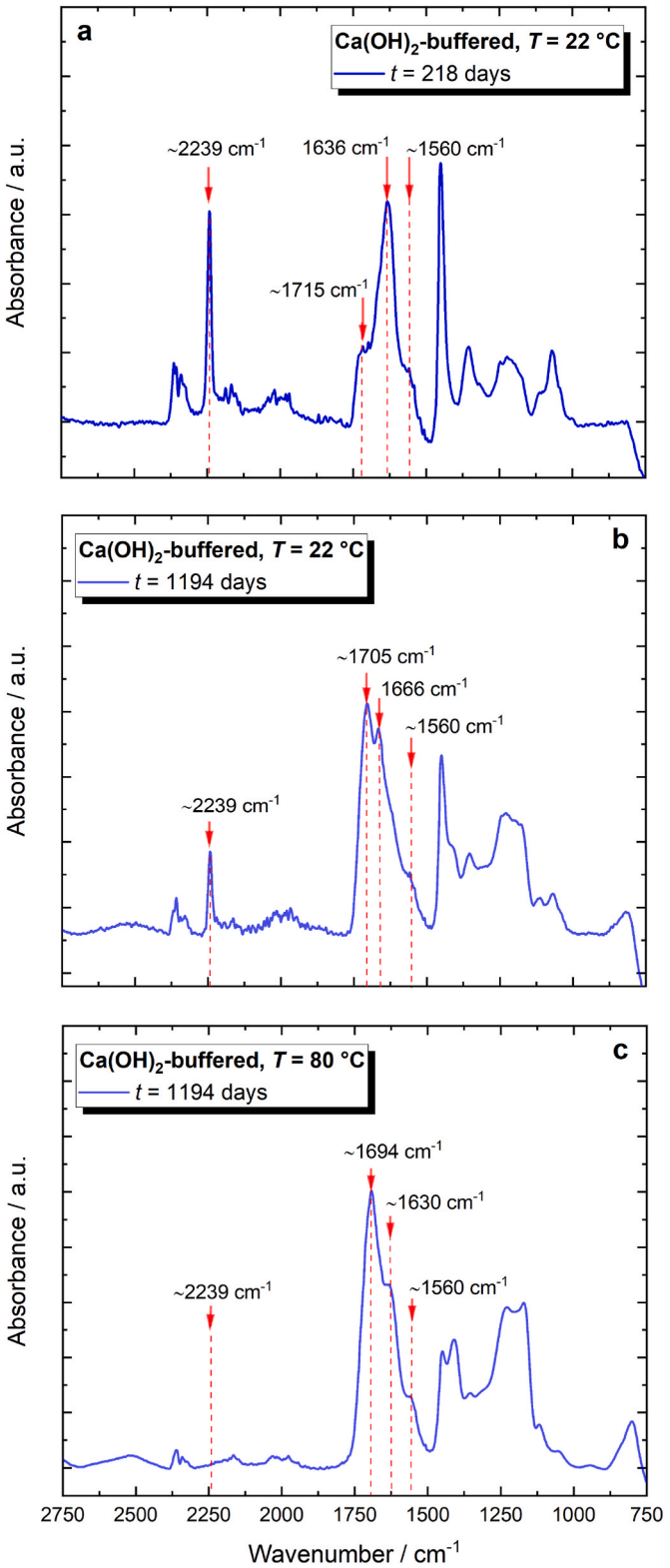

Fig. 9. Solid state FT-IR spectra of washed UP2 material degraded in $Ca(OH)_2$-buffered systems: **(a)** equilibrated at T = 22 °C for t = 218 days; **(b)** equilibrated at T = 22 °C for t = 1194 days; **(c)** equilibrated at T = 80 °C for t = 1194 days.

functional groups, respectively.

FT-IR spectra of the UP2W material collected at various stages of the $Ca(OH)_2$-buffered degradation experiments (t = 218 and 1194 days) are shown in Fig. 9. This figure shows a clear decrease of the feature at 2239

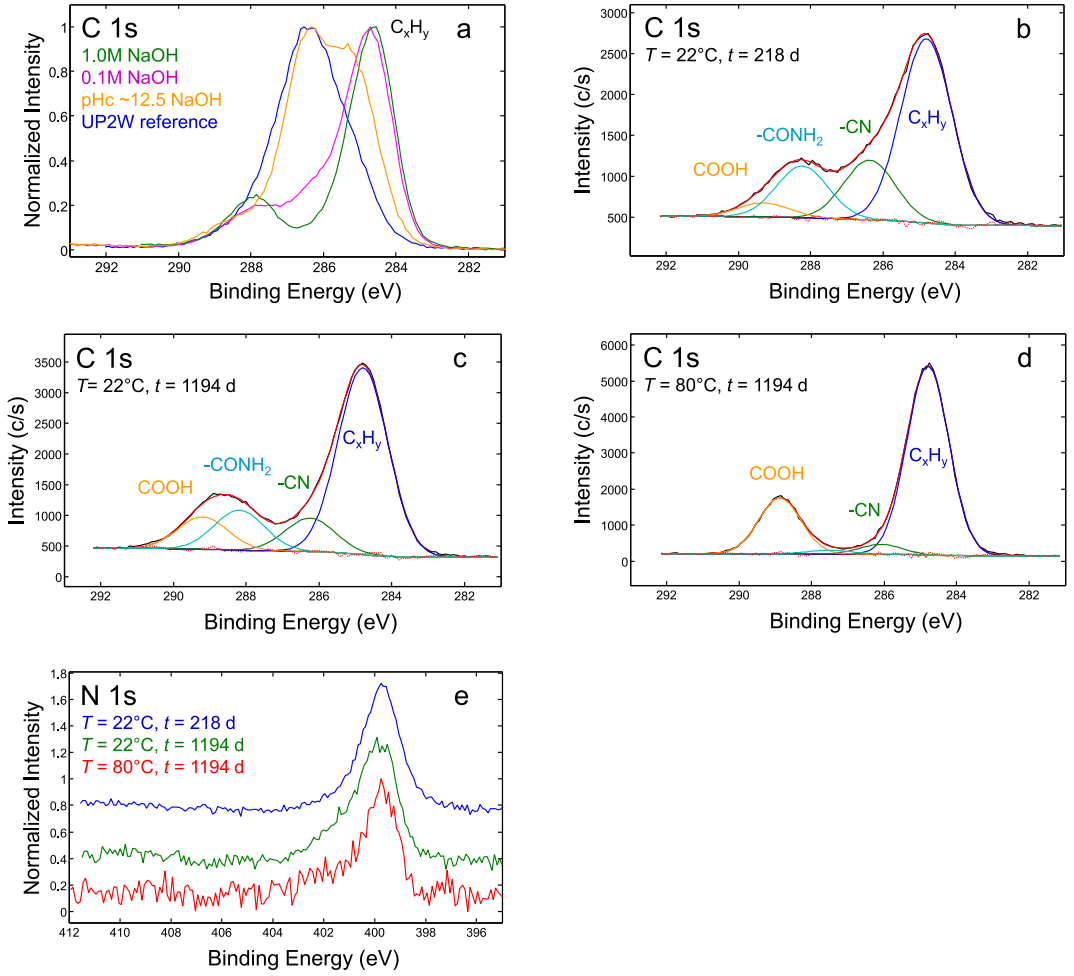

Fig. 10. XPS spectra on washed UP2W solid phases retrieved at different contact times in $Ca(OH)_2$-buffered systems: **(a)** C 1s elemental lines of original UP2W material (blue), and after equilibration in NaOH solutions 0.03 M (pH = 12.5, orange), 0.1 M (pink) and 1.0 M (green) at t = 740 days of contact time **(b)** curve fit of C 1s; T = 22 °C at 218 days; **(c)** curve fit of C 1s; T = 22 °C at 1194 days; **(d)** curve fit of C 1s; T = 80 °C at 1194 days; **(e)** combined N 1s elemental lines of all previously mentioned solids.

cm^{-1} (C≡N stretching) from $t = 218$ (Fig. 9a) to 1194 (Fig. 9b) days at $T = 22$ °C, confirming the progression of the PAN hydrolysis also in $Ca(OH)_2$-buffered systems. Note further that the signal of the nitrile-group vanishes at $t = 1194$ days for the $Ca(OH)_2$-buffered sample at $T = 80$ °C (Fig. 9c), thus underpinning the greater hydrolysis rate at elevated temperature. Consistently with the decrease of the nitrile signal, a systematic increase of the amide and carboxylate patterns within ~1560–~1705 cm^{-1} takes place. Deviations in the peak positions of the amide and carboxylate groups observed in $Ca(OH)_2$-buffered systems are consistent with previous studies available in the literature, which reported a shift on the carbonyl stretching frequency in amides and carboxylate asymmetric and symmetric stretching frequencies driven by complexation with divalent metal ions (Cu, Ca, Mn, Cd, Zn, Pb) (Otero et al., 2014; Robinet and Corbeil, 2003).

These observations support that hydrolysis of nitrile groups and scission reactions of PAN are decoupled in Ca-bearing systems. Hence, whilst a significant progress in the hydrolysis of the nitrile groups takes place in the solid material, the scission of PAN chains and consequent release of soluble fragments (as quantified by NPOC) remain limited.

3.2.2. XPS

Fig. 10a shows the C 1s elemental line of XPS spectra for the UP2W samples equilibrated in 0.03 (pH = 12.5), 0.1 and 1.0 M NaOH solutions for a contact time of 740 days. The results support that the extent of the nitrile-group hydrolysis follows the sequence 0.03 M NaOH (pH = 12.5) < 0.1 M NaOH <1.0 M NaOH, with the signal of amide and carboxylic carbon atoms mostly visible for samples equilibrated in 0.1 and 1.0 M NaOH. This is in line with FT-IR and NPOC measurements, suggesting faster hydrolysis and scission rates with increasing NaOH concentrations. These XPS observations are also in line with previous hydrolysis studies in NaOH-systems, which nevertheless reported significantly faster hydrolysis in the conditions of the corresponding degradation studies, *i.e.*, 1.5 M NaOH at $T = 45$ °C (Pérez-Alvarez et al., 2019) or 5 M NaOH at $T = 50$ °C (Jin et al., 2017; Lee et al., 2017).

Fig. 10b–d shows the curve fit of the C 1s elemental line of XPS spectra collected for the UP2W samples equilibrated in $Ca(OH)_2$-buffered solutions at $T = 22$ °C (Fig. 10b and c) and $T = 80$ °C (Fig. 10d). Fig. 10b shows that already after 218 days, a significant fraction of the original –CN groups (286.3 eV) converted into (mostly) $–CONH_2$ (288.2 eV) and (to less extent) –COOH (289.2 eV). For the same system but longer contact time (1194 days, see Fig. 10c), the fraction of –CN groups further decreases, with the consequent increase of the $–CONH_2$ and –COOH features. This trend is further confirmed for the $Ca(OH)_2$-buffered system equilibrated at $T = 80$ °C for 1194 days (Fig. 10d), which shows almost the full conversion of the nitrile group into carboxylate. This observation is consistent with the results obtained by FT-IR (see Section 3.2.1). The evolution of hydrolysis with time and the effect of temperature in the $Ca(OH)_2$-buffered systems is further confirmed in the

N 1s elemental line of the XPS spectra in Fig. 10e, which show the systematic decrease in the intensity of the –CN signal (reflected by a significant decrease in the signal-to-noise ratio in the normalized spectra). The comparison of the FT-IR and XPS results with NPOC data (see Section 3.1) strongly suggests that the extent of the conversion of the nitrile groups into carboxylates in PAN does not directly correlate with the cleavage/scission reaction, which is responsible for the release of soluble organic components into the aqueous phase.

The comparison of XPS and NPOC results in $Ca(OH)_2$- and NaOH-systems shows that although the hydrolysis of nitrile groups results in the ultimate formation of carboxylate groups in both systems, the dissolution process is hindered in the presence of Ca. We hypothesize that this could be caused by the complexation of Ca^{2+}-ions by the carboxylate and amide groups, which shifts the electron-density from the methine carbon, resulting in a lower probability for the proton, thus slowing down the scission of the polymer chains. Note that the adsorption of divalent metal ions by hydrolyzed PAN (*e.g.*, Pb^{2+}, Cu^{2+}, Cd^{2+}, Ni^{2+}, Co^{2+}, etc.) has been previously described in the literature (Deng et al., 2003; Lee et al., 2017).

3.3. Definition of proxy ligands for the degradation products of UP2W

In the early stages of this project, the need of defining proxy ligands for the degradation products of UP2W was discussed in the context of the sorption experiments that were to be conducted within Tasks 3 and 4 of WP CORI, dedicated to cement–organic and cement–radionuclide–organic interactions, respectively. The experimental strategy included a first series of sorption experiments with proxy ligands for the UP2W degradation products, to be complemented in a later stage of the project by sorption experiments involving degradation leachates generated in long-term degradation experiments with UP2W in $Ca(OH)_2$-buffered systems. For the selection of the proxy ligands, the following inputs were considered.

– ^{13}C NMR data available by the time of this assessment (1.0 M NaOH, $t = 425$ days; see Section 3.1.2), indicating: (i) the only presence of aliphatic C (no aromatic C); (ii) the full hydrolysis of the nitrile groups; (iii) the predominance of amide and carboxylate functional groups. Moreover, following mechanistic considerations in the literature (Litmanovich and Platé, 2000), the ultimate, full conversion of all amide groups into carboxylate groups is expected in the hyperalkaline conditions defined by cementitious environments.

- Compounds identified by Duro and co-workers in UP2W degradation leachates generated at pH = 12.5 and 13.4 by means of GC-MS (after transformation into butyl esters) (Duro et al., 2012). The list of compounds included: 3-hydroxybutanoic acid, 1,2,3,4-tetrahydronaphtalene, p-nitrotoluene, 4-phenyl-3-buten-2-one, malonic acid, methylmalonic acid, glutaric acid, 2-hydroxy-2-phenyletanoic acid, adipic acid, 3-methyladipic acid, 1,5-diphenyl-1,4-pentadien-3-one and 1,5-diphenyl-1-penten-3-one. All aromatic compounds in this list were disregarded in the selection of the proxy ligands because of incompatibility with ^{13}C NMR data obtained in this work.
- Organic ligands containing alcohol groups in α- and β-positions with respect to a carboxylic group have been shown to form particularly stable complexes with radionuclides in alkaline to hyperalkaline conditions, *e.g.*, isosaccharinic or gluconic acids (Hummel et al., 2005; Rai and Kitamura, 2017; Rojo et al., 2013; Tits et al., 2005; Vercammen et al., 2001). Thus, this combination of functional groups was favored in the selection of the proxy ligands, considering also the compounds identified by Duro and co-workers. Note also that selecting ligands with strong potential for complexation provides a more conservative perspective in a L/ILW disposal context.

Based on the considerations above, three proxy ligands were selected (see Fig. 11). Glutaric acid is a dicarboxylic acid identified in Duro et al., which was selected as representative of the bulk chain of the PAN-polymer fragments generated during degradation (Duro et al., 2012). The C5 linear structure with two end-carboxylate groups can be traced back to the hydrolysis of two consecutive nitrile groups in the original PAN structure. Two monocarboxylate ligands with alcohol groups in α- (α-hydroxyisobutyric acid) and β- (3-hydroxybutyric acid) positions were also selected to simulate the effect of the end-groups in the degradation products/fragments. 3-Hydroxybutyric acid was previously identified by Duro and co-workers, whereas α-hydroxyisobutyric acid holds the same chemical formula as 3-hydroxybutyric acid but with the alcohol group in α-position. This variation aims at accounting for the different saturation of the ending, double carbon–carbon bonds after a successful chain scission (Markovnikov product and anti-Markovnikov product). Although highlighting the usefulness of such proxy ligands to understand the role of the different functional groups that can be expected in the UP2W degradation products, we acknowledge the complexity of real degradation leachates, which we showed herein the necessity to consider in the overall assessment of the impact of UP2W degradation products in the radionuclide retention.

In the context of the Work Package 3 CORI of the EURAD EU project, the impact of the proxy ligands described above on the solubility and sorption of selected radionuclides (Ni, Nd, Eu, Pu) was thoroughly investigated (Szabo et al., 2022a, 2022b, 2023a). Likewise, the effect of degradation leachates obtained in this degradation study after *ca.* 1100 days was investigated for the uptake of Ni, Eu and Pu by cement (Szabo et al., 2023b).

4. Summary and conclusions

The degradation of UP2W, a polyacrylonitrile-based material used in nuclear power plants, was comprehensively investigated under hyperalkaline, reducing conditions relevant for L/ILW disposal. Six degradation matrix solutions were considered: (1) $Ca(OH)_2$-saturated solution at $T = 22$ °C, (2) $Ca(OH)_2$-saturated solution at $T = 22$ °C, containing Fe (0) to impose reducing conditions, (3) $Ca(OH)_2$-saturated solution at $T = 80$ °C, (4) dilute NaOH solution (0.03 M, with pH adjustments to maintain pH = 12.5) at $T = 22$ °C, (5) 0.10 M NaOH at $T = 22$ °C and (6) 1.00 M NaOH at $T = 22$ °C. Experiments were conducted under Ar-atmosphere, and degradation leachates and degraded UP2W solid material were characterized up to 1838 days using a multimethod approach including NPOC measurements, ^{13}C NMR, LC-OCD-UVD-OND, FT-IR and XPS.

NPOC values determined in $Ca(OH)_2$-buffered systems remain very low (<10 ppm) for up to ~ 600 days, consistently with previous degradation studies. The concentration of dissolved organic carbon

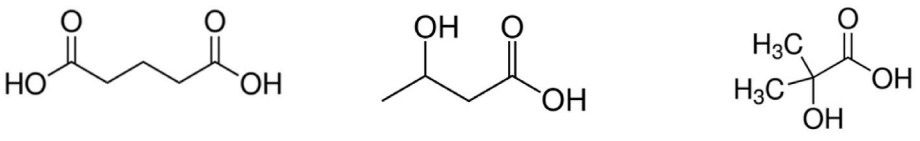

a **b** **c**

Fig. 11. Chemical structures of the proxy ligands for UP2W degradation products selected in this work: a. Glutaric acid (pentanedioic acid*); b. 3-Hydroxybutyric acid (3-hydroxybutanoic acid*); c. α-Hydroxyisobutyric acid (2-hydroxyisobutanoic acid*). Asterisk (*) denotes the IUPAC nomenclature for these compounds.

steadily increases at longer equilibration times, attaining ~30–50 ppm C at $t \approx 1800$ days. Significantly higher NPOC values with shorter induction times were quantified in NaOH systems, with an increasing trend following the increase in NaOH concentration. This observation confirms the key role of hydroxide in the degradation mechanism of PAN. The comparison of NPOC values in NaOH- and $Ca(OH)_2$-buffered systems with same pH (12.5) clearly shows that the presence of Ca has a strong hindering effect on the chain scission and release of soluble UP2W fragments.

The full conversion of nitrile groups into amide and carboxylate groups in the degradation leachates obtained in 1.0 M NaOH was confirmed by solution ^{13}C NMR. Information on the size distribution of the organic fragments in the degradation leachates was obtained by means of LC-OCD-UVD-OND. Large dissolved fragments (40 to > 65 kDa) were observed in all NaOH systems at contact times of $t \approx 700$ days. Significantly smaller fragments (<3 kDa) were identified in $Ca(OH)_2$-buffered systems equilibrated for the same time. A noticeable growth of these fragments was observed up to $t \approx 1800$ days, confirming that cross-linking of dissolved fragments is also a relevant process in $Ca(OH)_2$-buffered systems, in spite of the significantly lower dissolved organic content.

XPS and FT-IR characterization of solid phases equilibrated in NaOH solutions consistently showed the formation of significant fractions of amide and carboxylic groups, but also the presence of nitrile groups. This supports that nitrile hydrolysis of the bulk UP2W solid material remains incomplete after 5 years, in contrast to observations made for the degradation leachates. In $Ca(OH)_2$-buffered systems, XPS and FT-IR of UP2W degraded at $T = 22$ °C confirmed also the presence of nitrile groups in the solid material after 5 years, whereas the nitrile signal in the system equilibrated at $T = 80$ °C completely vanished after this time. This observation emphasizes the impact of temperature on the rate of hydrolysis of the nitrile groups in PAN. Shifts in the FT-IR signals of amide and carboxylate groups are attributed to the complexation with Ca, as previously reported in the literature for other divalent cations.

This study emphasizes the complexity of the degradation process of UP2W (and by extension PAN) in the hyperalkaline conditions defined by cement. Besides the hydrolysis reaction itself, chain scission and cross-linking reactions play a key role in the degradation process, particularly in the generation and stabilization of degradation leachates in the aqueous phase. The latter processes are particularly impacted by the presence of Ca, attributed to the complexation of Ca with amide and carboxylate groups in the hydrolyzed PAN-chain. This study provides a long-term perspective of the UP2W degradation, whilst giving new insights for the mechanistic interpretation of the different degradation steps.

CRediT authorship contribution statement

A. Tasi: Writing – review & editing, Writing – original draft, Supervision, Methodology, Investigation, Formal analysis, Data curation, Conceptualization. **P. Szabo:** Writing – review & editing, Investigation, Formal analysis, Data curation. **X. Gaona:** Writing – review & editing, Writing – original draft, Supervision, Project administration, Funding acquisition, Conceptualization. **M. Bouby:** Writing – review & editing, Methodology, Investigation, Formal analysis, Data curation. **T. Sittel:** Writing – review & editing, Investigation, Formal analysis, Data curation. **D. Schild:** Writing – review & editing, Investigation, Formal analysis, Data curation. **A.C. Maier:** Writing – review & editing, Validation, Project administration. **S. Hedström:** Writing – review & editing, Validation, Project administration, Conceptualization. **M. Altmaier:** Writing – review & editing, Project administration, Funding acquisition, Conceptualization. **H. Geckeis:** Writing – review & editing, Validation, Supervision, Conceptualization.

Declaration of competing interest

The authors declare the following financial interests/personal relationships which may be considered as potential competing interests: KIT-INE reports financial support was provided by European Union. KIT-INE reports financial support was provided by Swedish Nuclear Fuel and Waste Management Co. If there are other authors, they declare that they have no known competing financial interests or personal relationships that could have appeared to influence the work reported in this paper.

Data availability

Data will be made available on request.

Acknowledgements

The EURAD project leading to this application has received funding from the European Union's Horizon 2020 research and innovation programme under grant agreement No 847593. The work was performed in EURAD as part of the WP CORI and was partially funded by SKB. Klas Källström (SKB) is kindly acknowledged for his strong involvement in conceiving and conceptualising the study, as well as in the selection of the proxy ligands. The technical support of Yasmine Kouhail (KIT) with LC-OCD-UVD-OND measurements is highly appreciated. Jonas Rentmeister, Darlyn Rehhorn and Melanie Böttle (all KIT–INE) are gratefully acknowledged for the NPOC measurements and technical support.

Appendix A. Supplementary data

Supplementary data to this article can be found online at https://doi.org/10.1016/j.apgeochem.2024.106015.

References

Abdel Rahman, R.O., Metwally, S.S., El-Kamash, A.M., 2018. Life cycle of ion exchangers in nuclear industry: applications and management of spent exchangers. In: Torres Martinez, L.M., Kharissova, O.V., Kharisov, B.I. (Eds.), Handbook of Ecomaterials. Springer International Publishing.

Altmaier, M., Gaona, X., Fellhauer, D., Buckau, G., 2010. Intercomparison of Redox Determination Methods on Designed and Near-Neutral Aqueous Systems. KIT-SR 7572.

Bajaj, P., Chavan, R.B., Manjeet, B., 1985. Saponification kinetics of acrylonitrile terpolymer and polyacrylonitrile. J. Macromol. Sci., Chem. A22, 1219–1239.

Bajaj, P., Kumari, M.S., 1988. Structural investigations on hydrolyzed acrylonitrile terpolymers. Eur. Polym. J. 24, 275–279.

Bashir, Z., Manns, G., Service, D.M., Bott, D.C., Herbert, I.R., Ibbett, R.N., Church, S.P., 1991. Investigation of base induced cyclization and methine proton abstraction in polyacrylonitrile solutions. Polymer 32, 1826–1833.

Batty, N.S., Guthrie, J.T., 1981. A study of the origins of color in alkali degraded polyacrylonitrile and polymethacrylonitrile .3. Computer predicted structures for the degradation products. Macromolecular Chem. Phys.-Makromolekulare Chemie 182, 71–79.

Beamson, G., Briggs, D., 2012. The XPS of Polymers Database. SurfaceSpectra Ltd., Manchester, UK.

Brost, H.R., 1974. Filtering with Polyacrylonitrile or Polyamide Fibers as Filter Aid. US.

Bruno, J., González-Siso, M.R., Duro, L., Gaona, X., Altmaier, M., 2018. Key master variables affecting the mobility of Ni, Pu, Tc and U in the near field of the SFR repository. In: Main Experimental Findings and PA Implications of the PhD Thesis. SKB TR-18-01.

Chaudhary, B.K., Farrell, J., 2014. Preparation and characterization of homopolymer polyacrylonitrile-based fibrous sorbents for arsenic removal. Environ. Eng. Sci. 31, 593–601.

Choi, Y.H., Choi, C.M., Choi, D.H., Paik, Y., Park, B.J., Joo, Y.K., Kim, N.J., 2011. Time dependent solid-state ^{13}C NMR study on alkaline hydrolysis of polyacrylonitrile hollow fiber ultrafiltration membranes. J. Membr. Sci. 371, 84–89.

Dario, M., Molera, M., Allard, B., 2004. Effect of Organic Ligands on the Sorption of Europium on TiO_2 and Cement at High pH. SKB TR-04-04.

Deng, S.B., Bai, R.B., Chen, J.P., 2003. Behaviors and mechanisms of copper adsorption on hydrolyzed polyacrylonitrile fibers. J. Colloid Interface Sci. 260, 265–272.

Duro, L., Grive, M., Gaona, X., Bruno, J., Andersson, T., Boren, H., Dario, M., Allard, B., Hagberg, J., Källström, K., 2012. Study of the effect of the fibre mass UP2 degradation products on radionuclide mobilisation. SKB R-12-15.

Dyatlov, V.A., Grebeneva, T.A., Rustamov, I.R., Koledenkov, A.A., Kolotilova, N.V., Kireev, V.V., Prudskov, B.M., 2012. Hydrolysis of polyacrylonitrile in aqueous solution of sodium carbonate. Polym. Sci. B 54, 161–166.
Ermakov, I.V., Rebrov, A.I., Litmanovich, A.D., Plate, N.A., 2000. Alkaline hydrolysis of polyacrylonitrile, 1 - structure of the reaction products. Macromol. Chem. Phys. 201, 1415–1418.
Föchler, H.S., Mooney, J.R., Ball, L.E., Boyer, R.D., Grasselli, J.G., 1985. Infrared and NMR spectroscopic studies of the thermal-degradation of polyacrylonitrile. Spectrochim. Acta 41, 271–278.
Glazkovskii, Y.V., Mikhailov, P.V., 1966. A spectroscopic study of the structure of products of chemical transformations of polyacrylonitrile. Polym. Sci. 8, 1844–1849.
González-Siso, M.R., Gaona, X., Duro, L., Altmaier, M., Bruno, J., 2018. Thermodynamic model of Ni(II) solubility, hydrolysis and complex formation with ISA. Radiochim. Acta 106, 31–45.
Grenthe, I., Stumm, W., Laaksuharju, M., Nilsson, A.C., Wikberg, P., 1992. Redox potentials and redox reactions in deep groundwater systems. Chem. Geol. 98, 131–150.
Holgersson, S., Dubois, I., Börstell, L., 2011. Batch Experiments of Cs, Co and Eu Sorption onto Cement with Dissolved Fibre Mass UP2 in the Liquid Phase. SKB P-11-24.
Huber, S.A., Balz, A., Abert, M., Pronk, W., 2011. Characterisation of aquatic humic and non-humic matter with size-exclusion chromatography - organic carbon detection - organic nitrogen detection (LC-OCD-OND). Water Res. 45, 879–885.
Hummel, W., Anderegg, G., Rao, L., Puigdomènech, I., Tochiyama, O., 2005. Chemical Thermodynamics Vol. 9. Chemical Thermodynamics of Compounds and Complexes of U, Np, Pu, Am, Tc, Se, Ni and Zr with Selected Organic Ligands. Elsevier, North Holland, Amsterdam.
Jin, S.Y., Kim, M.H., Jeong, Y.G., Yoon, Y.I., Park, W.H., 2017. Effect of alkaline hydrolysis on cyclization reaction of PAN nanofibers. Mater. Des. 124, 69–77.
Keith-Roach, M., Lindgren, M., Källström, K., 2021. Assessment of Complexing Agent Concentrations for the Post-closure Safety Assessment in PSAR SFR. SKB R-20-04.
Kudryavtsev, Y.V., Krentsel, L.B., Bondarenko, G.N., Litmanovich, A.D., Platé, N.A., Schapowalow, S., Sackmann, G., 2000. Alkaline hydrolysis of polyacrylonitrile, 2 -: on the product swelling. Macromol. Chem. Phys. 201, 1419–1425.
Lee, S.H., Jeong, Y.G., Yoon, Y.I., Park, W.H., 2017. Hydrolysis of oxidized polyacrylonitrile nanofibrous webs and selective adsorption of harmful heavy metal ions. Polym. Degrad. Stabil. 143, 207–213.
Liang, C.Y., Krimm, S., 1958. Infrared spectra of high polymers .7. Polyacrylonitrile. J. Polym. Sci. 31, 513–522.
Litmanovich, A.D., Platé, N.A., 2000. Alkaline hydrolysis of polyacrylonitrile. On the reaction mechanism. Macromol. Chem. Phys. 201, 2176–2180.
Martin, S.C., Liggat, J.J., Snape, C.E., 2001. In situ NMR investigation into the thermal degradation and stabilisation of PAN. Polym. Degrad. Stabil. 74, 407–412.
Mathur, R.B., Bahl, O.P., Sivaram, P., 1992. Thermal-degradation of polyacrylonitrile fibers. Curr. Sci. India 62, 662–669.
Ochs, M., Mallants, D., Wang, L., 2016. Radionuclide and metal sorption on cement and concrete. Topics in Safety, Risk, Reliability and Quality, first ed. Springer International Publishing: Imprint: Springer, Cham, p. 1. online resource (XXX, 301 pages).
Otero, V., Sanches, D., Montagner, C., Vilarigues, M., Carlyle, L., Lopes, J.A., Melo, M.J., 2014. Characterisation of metal carboxylates by Raman and infrared spectroscopy in works of art. J. Raman Spectrosc. 45, 1197–1206.
Pérez-Alvarez, L., Ruiz-Rubio, L., Moreno, I., Vilas-Vilela, J.L., 2019. Characterization and optimization of the alkaline hydrolysis of polyacrylonitrile membranes. Polym. Bull. (Heidelberg, Ger.) 11.
Rai, D., Kitamura, A., 2017. Thermodynamic equilibrium constants for important isosaccharinate reactions: a review. J. Chem. Thermodyn. 114, 135–143.
Robinet, L., Corbeil, M.C., 2003. The characterization of metal soaps. Stud. Conserv. 48, 23–40.
Rojo, H., Tits, J., Gaona, X., Garcia-Gutierrez, M., Missana, T., Wieland, E., 2013. Thermodynamics of Np(IV) complexes with gluconic acid under alkaline conditions: sorption studies. Radiochim. Acta 101, 133–138.
Schurz, J., 1958. Discoloration effects in acrylonitrile polymers. J. Polym. Sci. 28, 438–439.
Seah, M.P., Gilmore, L.S., Beamson, G., 1998. XPS: binding energy calibration of electron spectrometers 5 - Re-evaluation of the reference energies. Surf. Interface Anal. 26, 642–649.
Sebesta, F., John, J., Motl, A., 1996. Phase II Report on the Evaluation of Polyacrylonitrile (PAN) as Binding Polymer for Absorbers Used to Treat Liquid Radioactive Wastes. SAND96-1088.
Surianarayanan, M., Vijayaraghavan, R., Raghavan, K.V., 1998. Spectroscopic investigations of polyacrylonitrile thermal degradation. J. Polym. Sci., Polym. Chem. Ed. 36, 2503–2512.
Szabo, P., Tasi, A., Gaona, A., Maier, A., Hedström, S., Altmaier, M., Geckeis, H., 2022a. Uptake of selected organic ligands by hardened cement paste: studies on proxy ligands for the degradation of polyacrylonitrile and general considerations on the role of different functionalities in the uptake process. Front. Nuclear Eng. 1, 997398.
Szabo, P., Tasi, A., Gaona, A., Polly, R., Maier, A., Hedström, S., Altmaier, M., Geckeis, H., 2022b. Solubility of Ca(II), Ni(II), Nd(III) and Pu(IV) in the presence of proxy ligands for the degradation of polyacrylonitrile in cementitious systems. Dalton Trans. 51, 9432–9444.
Szabo, P., Tasi, A.G., Gaona, X., Maier, A.C., Hedström, S., Altmaier, M., Geckeis, H., 2023a. Uptake of Ni(II), Eu(III) and Pu(III/IV) by hardened cement paste in the presence of proxy ligands for the degradation of polyacrylonitrile. Front. Nuclear Eng. 2, 1117413.
Szabo, P.G., Tasi, A.G., Gaona, X., Maier, A.C., Hedström, S., Altmaier, M., Geckeis, H., 2023b. Impact of the degradation leachate of the polyacrylonitrile-based material UP2W on the retention of Ni(II), Eu(III) and Pu(IV) by cement. Dalton Trans. 52, 13324–13331.
Tasdigh, H., 2015. Assessment of the Impact of Fiber Mass UP2 Degradation Products on nickel(II) and europium(III) Sorption onto Cement. KTH.
Tasi, A., Gaona, X., Fellhauer, D., Böttle, M., Rothe, J., Dardenne, K., Polly, R., Grivé, M., Colas, E., Bruno, J., Källström, K., Altmaier, M., Geckeis, H., 2018a. Thermodynamic description of the plutonium - alpha-D-isosaccharinic acid system I: solubility, complexation and redox behavior. Appl. Geochem. 98, 247–264.
Tasi, A., Gaona, X., Fellhauer, D., Böttle, M., Rothe, J., Dardenne, K., Polly, R., Grivé, M., Colas, E., Bruno, J., Källström, K., Altmaier, M., Geckeis, H., 2018b. Thermodynamic description of the plutonium - alpha-D-isosaccharinic acid system II: formation of quaternary Ca(II)-Pu(IV)-OH-ISA complexes. Appl. Geochem. 98, 351–366.
Tits, J., Wieland, E., 2018. Actinide Sorption by Cementitious Materials. PSI Bericht Nr, vols. 18–02.
Tits, J., Wieland, E., Bradbury, M.H., 2005. The effect of isosaccharinic acid and gluconic acid on the retention of Eu(III), Am(III) and Th(IV) by calcite. Appl. Geochem. 20, 2082–2096.
Truong, N.D., Galin, J.C., Francois, J., Pham, Q.T., 1986a. Microstructure of acrylamide acrylic-acid copolymers .1. As obtained by alkaline-hydrolysis. Polymer 27, 459–466.
Truong, N.D., Galin, J.C., Francois, J., Pham, Q.T., 1986b. Microstructure of acrylamide acrylic-acid copolymers .2. As obtained by direct copolymerization. Polymer 27, 467–475.
UP2W, 2017. Material safety datasheet. Aqua Chem, Milan (Italy). (Accessed 8 June 2017).
Vercammen, K., Glaus, M.A., Van Loon, L.R., 2001. Complexation of Th(IV) and Eu(III) by alpha-isosaccharinic acid under alkaline conditions. Radiochim. Acta 89, 393–401.
Wang, Y.S., Xu, L.H., Wang, M.Z., Pang, W.M., Ge, X.W., 2014. Structural identification of polyacrylonitrile during thermal treatment by selective ^{13}C labeling and solid-state ^{13}C NMR spectroscopy. Macromolecules 47, 3901–3908.
Wieland, E., 2014. Sorption Data Base for the Cementitious Near Field of L/ILW and ILW Repositories for Provisiona Safety Analyses for SGT-E2. Nagra Technical Report 14-08.
Yalcintas, E., Gaona, X., Scheinost, A.C., Kobayashi, T., Altmaier, M., Geckeis, H., 2015. Redox chemistry of Tc(VII)/Tc(IV) in dilute to concentrated NaCl and MgCl2 solutions. Radiochim. Acta 103, 57–72.
Zahn, H., Schäfer, P., 1959. Über Oligomere.16. Zur Kenntnis der Oligomeren des Acrylnitrils. 2. Mitt. Polymerisations- und Abbauversuche. Makromol. Chem. 30, 225–237.